Meat and Muscle Biology™

Prediction of Carcass Composition and Meat and Fat Quality Using Sensing Technologies: A Review

P. L. A. Leighton[1], J. Segura[1], S. Lam[1], M. Marcoux[2], X. Wei[1,3], O. Lopez-Campos[1], P. Soladoye[1], M. E. R. Dugan[1], M. Juarez[1], and N. Prieto[1]*

[1]Lacombe Research and Development Centre, Agriculture and Agri-Food Canada, Lacombe, Alberta, Canada
[2]Sherbrooke Research and Development Centre, Agriculture and Agri-Food Canada, Sherbrooke, Quebec, Canada
[3]Food Science Department, University of Guelph, Guelph, Ontario, Canada
*Corresponding author. Email: nuria.prietobenavides@agr.gc.ca (N. Prieto)

Abstract: Consumer demand for high-quality healthy food is increasing; therefore, meat processors require the means to assess their products rapidly, accurately, and inexpensively. Traditional methods for quality assessments are time-consuming, expensive, and invasive and have potential to negatively impact the environment. Consequently, emphasis has been put on finding nondestructive, fast, and accurate technologies for product composition and quality evaluation. Research in this area is advancing rapidly through recent developments in the areas of portability, accuracy, and machine learning. Therefore, the present review critically evaluates and summarizes developments of popular noninvasive technologies (i.e., from imaging to spectroscopic sensing technologies) for estimating beef, pork, and lamb composition and quality, which will hopefully assist in the implementation of these technologies for rapid evaluation/real-time grading of livestock products in the near future.

Key words: computed tomography, dual-energy X-ray absorptiometry, computer vision systems, ultrasound and bioelectrical impedance analysis, near infrared and Raman spectroscopy, hyperspectral imaging
Meat and Muscle Biology 5(3): 12951, 1–21 (2021) **doi:10.22175/mmb.12951**
Submitted 30 June 2021 Accepted 14 September 2021

This paper was accepted as a contribution to the 2021 AMSA Reciprocal Meat Conference.

Introduction

Consumer demand is one of the most important factors influencing livestock carcass value. Meat consumption drivers are complex and are influenced by interrelated factors. Apart from price, eating satisfaction, sensory characteristics, and nutrient content are key factors influencing purchase decisions for fresh meat (Grunert et al., 2004). However, many of these factors are not taken into consideration using current carcass grading systems, and consumers from medium to high incomes are becoming increasingly more discerning and willing to pay for both credence and measurable quality differences (Meyerding et al., 2018; Froehlich et al., 2009). Consequently, opportunities for adding value are not being realized, and producers are not receiving appropriate feedback to improve feeding and breeding strategies.

Carcass classification and grading systems are employed to provide a better understanding of livestock products and markets trends, as well as to guarantee product quality and homogeneity, thereby ensuring competitiveness (Polkinghorne and Thompson, 2010). However, these procedures are still largely performed by graders using traditional manual evaluation techniques. Since the implementation of the earliest grading systems, it has been difficult to devise objective carcass assessments that accurately and precisely predict meat yield while maintaining packing plant hygiene and line speed. Within this environment, there would also be no option to use conventional methods to comprehensively evaluate meat and fat quality at line speed, because these methods are expensive, time-consuming, destructive, and sometimes hazardous to health or the environment (Prieto et al., 2009; Yancey et al., 2010). As a result, in order to address current market scenarios and global environmental challenges, the implementation of real-time noninvasive technologies that use sensors to predict carcass composition and meat and fat quality are quickly evolving to precisely predict detailed product attributes and are helping to optimize product evaluations.

Several comprehensive reviews have been published on the application of sensing technologies for quantitatively and qualitatively predicting carcass composition and meat quality (Aalhus et al., 2014; Prieto et al., 2017, 2018b; Tao and Ngadi, 2018; Kutsanedzie et al., 2019; López-Campos et al., 2019). Nevertheless, recent advances in instrumentation (e.g., portable and handheld devices) together with increased computing power and more advanced statistical approaches (e.g., machine learning algorithms) have expanded the use of sensing technologies for predicting composition and quality. The current review will thus critically evaluate and summarize the most relevant and recent studies applying sensing technologies to predict carcass composition (computed tomography [CT], dual-energy X-ray absorptiometry [DXA], computer vision systems [CVS], ultrasound [US], and bioelectrical impedance analysis [BIA]) and meat and fat quality (near infrared spectroscopy [NIRS], hyperspectral imaging [HSI], and Raman spectroscopy).

Technologies for Carcass Composition Evaluation

Computed tomography

X-ray–based technologies for assessing carcass composition are based on differences in signal attenuation when X-rays pass through different tissues. Basically, body components with strong absorbance, such as bones, appear bright and light, and elements that do not absorb the X-rays appear dark (Narsaiah et al., 2019). Traditional X-ray radiography is in 2 dimensions (2D), and 3D scanning was made possible through CT, wherein either samples rotate on a translation stage or the equipment rotates around the sample (spiral CT).

The application of CT for measuring lean, fat, and bone has been largely described and reviewed (Olsen et al., 2017; López-Campos et al., 2019). Recently, a number of studies have reported the application of CT in live animals for the estimation of body tissue composition. In this context, Pan et al. (2021) used automated CT segmentation in live pigs together with deep neural network statistical analysis and reported accurate predictions for body fat, lean, and bone weights (coefficients of determination: $R^2 = 0.94$, 0.86, and 0.91, respectively). In turn, Geraldo et al. (2021) found high predictability for body tissue composition of the Santa Inés breed of sheep (R^2 of prediction: $R^2_{\mathrm{p}} = 0.90$, 0.81, and 0.81 for fat, lean and bone weights, respectively), using CT scans together with the Cavalieri method (Gundersen et al., 1988) of multiple linear regression (MLR) analysis.

Apart from traditional studies on estimation of carcass tissue composition, Font-i-Furnols et al. (2021) used CT technology in both live dairy calves and carcasses to estimate carcass fat, moisture, and protein content. These authors found that prediction for carcass fat content was moderate when scanning live calves and high when scanning carcasses ($R^2_{\mathrm{p}} = 0.69$ and 0.88, respectively), whereas predictability for moisture ($R^2_{\mathrm{p}} = 0.36$ and 0.59) and protein content ($R^2_{\mathrm{p}} = 0.36$ and 0.26) was low in both scanning modes. Font-i-Furnols et al. (2019) used CT in live pigs to estimate the intramuscular fat (IMF) content in different pig muscles; however, the predictions were not accurate (R^2 of cross-validation: $R^2_{\mathrm{cv}} = 0.07$ to 0.42).

Dual-energy X-ray absorptiometry

DXA is based on differential absorption of X-rays of varying energy levels by different tissues. In comparison to CT, DXA has some advantages in that it is less expensive in terms of instrument and installation costs and requires minimal radiation exposure.

In research abattoirs, recent studies have reported potential for DXA to be able to predict not only whole carcass but also primal and retail cut composition, using conventional manual cut-outs as the reference method. Using linear regression analysis, Kipper et al. (2019) reported high DXA predictability in pork for total side weight ($R^2 = 0.97$ to 0.99); total bone ($R^2 = 0.76$ to 0.95), fat ($R^2 = 0.96$ to 0.99), and lean ($R^2 = 0.84$ to 0.98) content; and tissue composition of primal cuts ($R^2 = 0.76$ to 0.99), although accuracy varied depending on factors such as the region of interest selected, carcass weight, and/or the selected prediction equation. These authors suggested that the regions of interest should be chosen based on the item to be analyzed in order to decrease the error of analysis. In beef, López-Campos et al. (2018) scanned steer primals using DXA and reported a high accuracy for predicting total lean ($R^2_{\mathrm{p}} = 0.99$), fat ($R^2_{\mathrm{p}} = 0.98$), and bone ($R^2_{\mathrm{p}} = 0.94$) in whole carcasses using partial least squares regression (PLSR), as well as the tissue composition from 12 out of 15 retail cuts ($R^2_p = 0.81$ to 0.95) (Figure 1). Similarly, high predictability by DXA in cull cows was obtained by Segura et al. (2021) for total lean, fat, and bone content in the whole carcass ($R^2_p = 0.99$, 0.99, and 0.92, respectively) and tissue composition of most individual cuts ($R^2_p = 0.74$ to 0.99). However, lower predictability was found for bone estimation in the flank retail cut ($R^2_p = 0.31$), probably because of the high variability in both DXA estimations and weight measurements, as a consequence of the low amount of bone included in this primal. Additionally, R^2_p values of 0.86 and 0.81 were described for retail cut and lean meat yield percentages, respectively.

Some of the latest developments in DXA have focused on its online application. In this context, Gardner et al. (2018) reported satisfactory prediction models for total fat, lean, and bone in lamb carcasses ($R^2_p = 0.89$, 0.69, and 0.68, respectively), using a unit installed at a commercial abattoir at line speed. Likewise, using online DXA at commercial abattoirs, high predictability was reported in lamb by Connaughton et al. (2020b) for carcass fat, lean, and bone across varying processing factors ($R^2_p =$ 0.81 to 0.95) and by Connaughton et al. (2020a) for carcass fat and lean content considering a range of phenotypic and genotypic variables ($R^2_p = 0.91$ and 0.74, respectively). Additionally, Gardner et al. (2021), also using an online DXA unit installed at a commercial abattoir, reported accurate predictions ($R^2_p = 0.63$ to 0.95) for several retail cut weights in lambs. In beef, Calnan et al. (2021) have recently developed a prototype of a rapid DXA in a shipping container and reported high predictability for lean, fat, and bone of entire carcass sides ($R^2_p = 0.85$, 0.94, and 0.82, respectively) and forequarters ($R^2_p =$ 0.83, 0.93, and 0.82, respectively) and moderate accuracy for hindquarters ($R^2_p = 0.68$, 0.80, and 0.73, respectively). It is important to note that, in all studies, CT was used as the standard method for calibration purposes; however, DXA technology is also becoming a reference technology for research studies on growth performance and carcass composition evaluation (Sousa dos Santos et al., 2021). Commercial application of DXA has now also been extended to use with robotic arms (Scott Technology

Figure 1. Beef chuck primal cut scanned with an iDXA unit and X-ray image generated (Lopez-Campos et al. 2018). Source: Agriculture and Agri-Food Canada–Lacombe Research and Development Centre.

Ltd., Dunedin, New Zealand) for further carcass processing at high line speeds.

Beyond use to estimate carcass composition, a number of authors have either suggested the application of or successfully implemented DXA to allow for precision nutrition/feeding of ruminants (González et al., 2018), as a methodology for estimating growth performance and body protein mass in growing-finishing pigs (Remus et al., 2020) and to predict aspects of lamb eating quality using bone DXA values (Anderson et al., 2021).

Computer vision systems

CVS—also known as machine vision systems, visual image systems, or just image systems—are based on sequential image acquisition, image processing (thresholding, binarization, etc.), image analysis (image segmentation, feature extraction, etc.), and data analysis (data normalization, model fitting, validation and tuning, prediction, etc.). The CVS have been applied in diverse areas to describe different characteristics through images by interpreting, reconstructing, and extracting properties (shapes, textures, densities, distances, etc.).

In livestock and meat science, CVS have mainly been applied to estimate carcass composition and quality for carcass classification and grading purposes. Lohumi et al. (2018) found predictions with moderate accuracy for lean meat yield ($R^2_p = 0.77$) in commercial pork carcasses using images obtained from a fully automated VCS2000 camera (e+v® Technology GmbH, Oranienburg, Germany) installed in a commercial slaughterhouse and MLR analyses. Additionally, in this study, the lean meat yield predictability was relatively high for main cuts such as ham, belly, and shoulder ($R^2_p = 0.80$, 0.89, and 0.85, respectively) and moderate for loin and tenderloin ($R^2_p = 0.73$ and 0.67, respectively). In beef, Segura et al. (2021) demonstrated the feasibility of using the variables from a combination of VBS2000 (whole-side carcass camera: e+v® Technology GmbH, Oranienburg, Germany) and VBG2000 (rib-eye camera: e+v® Technology GmbH, Oranienburg, Germany) cameras along with PLSR analysis to accurately predict carcass tissue composition ($R^2_p = 0.84$ to 0.93) and tissue composition of most individual cuts ($R^2_p = 0.71$ to 0.88), as well as lean meat and retail cut yield ($R^2_p = 0.90$ and 0.86, respectively) (Figures 2 and 3). Regarding lamb, the ability of CVS to predict carcass commercial cut weight and yield of light lambs was evaluated by Batista et al. (2021). The results of this study confirmed previous reports on the ability of CVS technology to estimate the weights of different cuts ($R^2_{cv} = 0.96$ to 0.99) and their lean meat yields ($R^2_{cv} = 0.96$ to 0.99), whereas the accuracy was more limited for predicting cut weight ($R^2_{cv} < 0.43$) and lean meat in percentage ($R^2_{cv} < 0.44$).

Apart from carcass quality estimations, CVS have also been used to predict meat quality. In this context, Araújo et al. (2020) evaluated the relationships between carcass shape, carcass tissue characterization, and commercial cuts of hair sheep lambs to predict meat quality ($R^2_p = 0.82$), suggesting the potential of the technology to establish categories for carcass classification in lambs. In fact, Stewart et al. (2021) observed accurate predictions for rib-eye area ($R^2 = 0.83$), Meat Standards Australia marbling ($R^2 = 0.76$), AUS-MEAT marbling ($R^2 = 0.70$), and chemical IMF ($R^2 = 0.78$) using a prototype vision system on a phenotypically diverse beef and lamb carcass population.

The industry's need for automation and robotization, coupled with the concept of data objectivity without human intervention, have fostered interest in the development and use of 3D vision technologies (Vázquez-Arellano et al., 2016). In this context, Le Cozler et al. (2019b) demonstrated the potential of using laser cameras and image analysis to objectively predict body weight ($R^2_p = 0.93$), total volume ($R^2_p = 0.99$), and area ($R^2_p = 0.90$) of dairy cows. In a second study, using the same laser cameras, Le Cozler et al. (2019a) also tested the feasibility of this technology for assessing animal morphology, namely heart girth, chest depth, and wither height as well as hip, backside, and ischial widths ($R^2_p = 0.38$ to 0.79). A number of systems incorporating 3D CVS have been approved in Europe to estimate meat yield and grading in pork carcasses (Implementing Decisions of European Commission [2011] and European Commission [2019]). For instance, the Frontmatec company (Kolding, Denmark) has developed a 360° 3D scanning system—the Beef Classification Center BCC-3TM—which recreates a complete beef half-carcass. The system provides data to estimate conformation and fattening level according to EUROP standards and has estimated with relatively high accuracy the weight of beef commercial cuts in a commercial abattoir ($R^2_{cv} = 0.78$, 0.85, and 0.81, for inside, knuckle, and rump, respectively; Esberg et al., 2019). Following a proof-of-concept using a 3D red, green, and blue camera, Alempijevic et al. (2021) reported an R^2_{cv} value of 0.69 to predict lean meat yield in beef at 2 commercial abattoirs.

In cattle, Miller et al. (2019) predicted live weight, cold carcass weight, and saleable meat yield with

Figure 2. Carcass side image taken with a whole-side carcass camera (Segura et al., 2021). Source: Agriculture and Agri-Food Canada–Lacombe Research and Development Centre.

moderate to high accuracy ($R^2_p = 0.70$, 0.88, and 0.72, respectively), using a 3D time-of-flight camera and machine learning algorithms (artificial neural networks) to extract 60 predictor variables from images of live steers and heifers collected at both commercial and research farms. In addition, the models predicted EUROP fat and conformation grades with 54% and 55% accuracy (R^2), respectively.

In pig carcasses, Masoumi et al. (2021) developed a method of digital imaging from full 3D models of half carcass sides and reported moderate predictability for the lean and fat content ($R^2_p = 0.77$ and 0.73, respectively) (Figure 4). However, predictability varied for the weight of 12 different commercial cuts ($R^2_p =$ 0.41 to 0.80). In the case of lambs, the application of 3D-CVS to estimate live weight has also been described by Samperio et al. (2021), reporting weight estimates of the animal with an error of less than 6%.

Recently, CVS has been applied to predict meat quality variables. For instance, Tomasević et al. (2019) reported that CVS colors were more accurate and precise in classifying bi-colored and non-uniformly colored beef and pork products (frequency of similarity ranged from 92.9% to 100%) and better mirrored their real color as perceived by panelists than a traditional colorimeter. In turn, Uttaro et al. (2021) developed an image analysis approach for identifying marbling on intact pork loin and reported a moderate estimation for IMF content, similar to both RAW ($R^2 = 0.72$) and JPEG ($R^2 = 0.72$) images. However, lower IMF predictability was reported at very high marbling levels.

Ultrasound

US is a nondestructive, cost-effective, easy-to-operate and reliable technology that provides in-depth measurements useful for evaluating carcass composition (Xiong et al., 2017). However, US measurements can be affected by different factors such as repeatability and reproducibility of the measures as consequences of operator performance (Vargas et al., 2021), position (transverse vs. longitudinal dorsal) (Cisneros et al., 1996), and pressure of the probe on live animals (Ripoll et al., 2009). To minimize these sources of error, many associations that assess the genetic potential of cattle in North America have certification policies through the

Figure 3. Rib-eye image analysis performed with a rib-eye camera system at the 12th-13th rib (Segura et al., 2021). Source: Agriculture and Agri-Food Canada–Lacombe Research and Development.

Ultrasound Guidelines Council (Tait, 2016). There is extensive literature on the use of US in animal husbandry and evaluation of carcass composition in different species (Pathak et al., 2011; Xiong et al., 2017; López-Campos et al., 2019). Nevertheless, recent studies have reported limitations of current commercial US devices, and new applications of high-intensity US (HIUS) to livestock end-products have emerged.

In many cases, the US devices provide an image that must be processed to extract useful information such as marbling (Fukuda et al., 2017) or fat and muscle thickness (Theriault et al., 2009). Nevertheless, owing to software advances, current commercial US devices can directly provide those measurements. Lucas et al. (2017) found that fat and muscle thickness obtained with a commercial US Piglog 105 device (Carometec A/S, Herlev, Denmark) in live pigs were highly and moderately correlated with the reference method (correlation coefficients: $r = 0.97$ and 0.65, respectively). Additionally, these authors successfully predicted carcass lean yield (R^2_p = 0.86). Using the same US equipment, Szyndler-N dza et al. (2016) estimated with moderate to high accuracy pig carcass lean yield ($R^2 = 0.51$ to 0.84) and lean weight ($R^2 = 0.40$ to 0.74) in different breeds. When all breeds were combined in the analysis, lower US predictability was reported for carcass lean yield and weight ($r = 0.63$ and 0.58, respectively), although lean yield estimation improved ($r = 0.71$) when breed was considered in the model. Using other automatic US systems installed on the slaughter line, Font-i-Furnols and Gispert (2009) found moderate predictions for pig carcass lean yield using 42 and 2 variables from AutoFOM (Frontmatec, Kloding, Denmark) and Ultrafom (SFK Technology A/S, Herlev, Denmark) devices in equation models ($R^2 =$ 0.78 and 0.64, respectively). Higher predictability

Figure 4. Assessment of pig half carcass composition using a novel 3D digital imaging approach (Masoumi et al., 2021). Source: Agriculture and Agri-Food Canada–Sherbrooke Research and Development Centre.

($R^2 = 0.93$, 0.82, 0.81) was observed by Janiszewski et al. (2019) for loin, ham, and belly lean yield, respectively, using 31 variables from AutoFOM, although lower US predictability was observed for other major cuts such as shoulder ($R^2 = 0.68$) and neck ($R^2 = 0.42$).

AutoFOM has also been used to estimate commercial cut weights. Choi et al. (2018) reported more accurate AutoFOM predictions for larger ($R^2_{cv} = 0.77$ to 0.86) compared with smaller commercial cut weights ($R^2_{cv} = 0.34$ to 0.57), which might be due to the lack of anatomical reference points and the lack of a strong correlation between the scanned area of the carcass and the smaller commercial cut weight. Nevertheless, the predictability obtained for heavier primal cuts shows US as an advantageous management tool enabling slaughterhouses to optimize product sorting prior to carcasses entering the cold room. Recently, Kress et al. (2020) estimated primal cut weights in different sex groups (gilts, boars, immunocastrates, and barrows) using an AutoFOM US device, and they concluded that the ability of the AutoFOM III estimation formulas to provide precise data for boars and immunocastrates is unclear. Particularly, boars might be misevaluated because of an increased proportion of lean meat and a different carcass composition due to sexual dimorphism. Hence, these authors suggested that the AutoFOM estimation formulas must be further examined in a detailed dissection trial and validation study in order to ensure fair pricing conditions for all sex groups and to avoid market distortions.

As biological tissue characteristics are sensitive to ultrasonic frequency (Park et al., 1994), HIUS has been applied recently to modify the physical and chemical properties of meat, in order to improve meat quality and safety. According to Jayasooriya et al. (2004), acoustic parameters such as frequency, intensity, duration of treatment, and temperature can influence the result from the ultrasonication. In this context, Diaz-Almanza et al. (2019) applied HIUS (37 kHz, 90 W cm^{-2}) at different exposure times (0, 10, 20, and 40 min) in beef *longissimus thoracis et lumborum* (LTL) and observed the highest ($P < 0.05$) tenderness at 40 min; however, microbial reduction was higher at 10 min. Peña-González et al. (2017) observed that lipid oxidation increased ($P < 0.0089$), shear force decreased ($P < 0.0001$), and meat was perceived as more tender and juicy in HIUS-treated beef *longissimus dorsi* (40 kHz, 11 W cm^{-2}, 60 min) after 14 d of storage.

Fallavena et al. (2020) applied HIUS at different temperatures (10°C to 35°C) and intensities (22 to 84 W cm^{-2}) on beef *biceps femoris* and observed that high temperature and US intensity resulted in less tenderness whereas intermediate US intensity and low temperatures improved meat tenderness ($P < 0.05$). Overall, HIUS reduced water-holding capacity (WHC) and had a negative effect on lipid oxidation but did not influence pH or color.

Bioelectrical impedance analysis

The basic principle of BIA is to introduce an alternating current (1–500 kHz) through a body (fat and muscle tissues) using 2 transmission electrodes, while the electrical resistance produced is measured by 2 detector electrodes at the opposite side of the body (Swantek et al., 1992) (Figure 5). The BIA is a nondestructive technology used for characterizing different biological tissues that has decisive benefits compared with other characterization methods, because it is more efficient owing to the relatively reduced time, hardware, and software required (Kanoun, 2018). Although BIA technology was evaluated several years ago for estimating lamb carcass composition (Berg and Marchello, 1994), interest in using and exploring the potential of this technology is ongoing.

Using BIA measurements collected *in vivo* from lambs, Moro et al. (2019) predicted carcass weight and yield at slaughter with high ($R^2_{cv} = 0.96$) and moderate ($R^2_{cv} = 0.57$) accuracy, respectively. Moro et al. (2020) successfully predicted both lean ($R^2_{cv} = 0.98$ and 0.99) and fat (kilograms) ($R^2_{cv} = 0.92$ and 0.91) content in lamb carcasses using BIA measurements collected at 50 kHz on hot and cold carcasses, respectively. An et al. (2021) reported high ($P < 0.01$) correlations between fat percentage obtained with a BIA device on live pigs and lean meat percentage ($r = -0.97$) or backfat thickness (millimeters) ($r = 0.93$) measured with US equipment, indicating that BIA technology might be useful for predicting body compositions of live finishing pigs to facilitate swine feed management.

Beyond the application of BIA to evaluate carcass composition, BIA measurements have been recently used to predict meat quality. In this context, Huh et al. (2021) recently demonstrated that multifrequency impedance measurements were significantly correlated with moisture, fat ($r = -0.83$ and 0.86 at 128 kHz, respectively), and protein ($r = -0.86$ at 80 kHz)

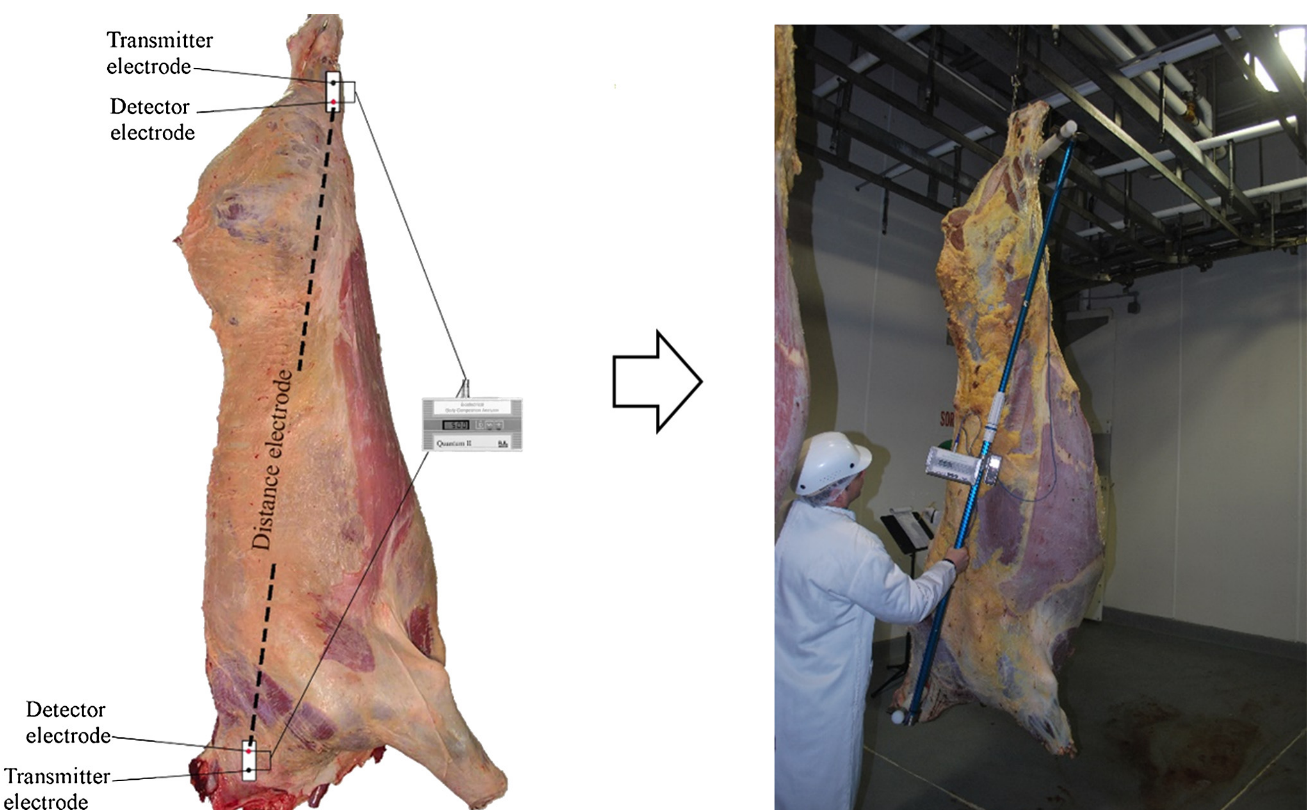

Figure 5. Bioelectrical impedance analysis applied to a beef carcass. Source: Agriculture and Agri-Food Canada–Sherbrooke Research and Development Centre.

content of beef. However, crude ash content was not associated with impedance values ($r < -0.43$). Afonso et al. (2020) found that BIA predictability was relatively high for IMF content ($R^2_{cv} = 0.79$) and low to moderate for collagen content and shear force value ($R^2_{cv} = 0.51$ and 0.60, respectively) in beef LTL muscle. They also reported low predictions for cooking loss, pH, and color values ($R^2_{cv} \leq 0.36$).

BIA spectroscopy is increasingly used for real-time measurements in portable and embedded solutions owing to favorable developments in the field of microelectronics. Nevertheless, despite the potential of BIA technology to evaluate the quality of carcasses and meat, some studies have emphasized the need to refine the use of BIA for acceptance and transfer to industrial environments (slaughterhouses, food processing cutting rooms, etc.) (Zhao et al., 2017; Afonso et al., 2020).

Technologies for Meat and Fat Quality Evaluation

Near infrared spectroscopy

In NIRS (12,500 to 4,000 cm^{-1} or 800 to 2,500 nm), there is a change in dipole moment during vibrational transitions of a molecule, resulting in absorption of an infrared photon by the molecule. The absorbed photon has the same amount of energy as the energy difference between the 2 vibrational states of the molecule (Agarwal and Atalla, 2010). The vibrations involve C–H, O–H, and N–H chemical bonds (Prieto et al., 2017). There are many advantages of NIRS over conventional methods for meat quality analysis. NIRS is a sensitive, fast, nondestructive, cost-effective, and environmentally friendly technology (Dixit et al., 2017). Additionally, NIRS has a higher penetration depth than other spectroscopic techniques (Hassoun et al., 2020). One disadvantage of NIRS, however, is that meat is composed of approximately 75% water, which is strongly absorbed in the infrared region and can influence NIRS predictions (Andueza et al., 2019).

Recently, NIRS has been used to predict the content of chemical components in intact meat samples. Dixit et al. (2020b) successfully predicted IMF content of intact beef LTL at 24 h postmortem using offline and online a portable visible (VIS)-NIR spectrometer (350 to 2,500 nm) in a commercial pilot plant and PLSR ($R^2_{p} = 0.88$ and 0.89, respectively). Patel et al. (2021) found moderate IMF ($R^2_{p} = 0.46$, 0.66, and 0.62) and moisture ($R^2_{p} = 0.51$, 0.63, and 0.70) content estimations for 7-d aged beef using a portable Vis-NIRS (350 to 1,830 nm), a portable NIRS (950 to 1,650 nm), and a handheld micro-NIRS (905 to 1,649 nm), respectively, in a research lab. Unexpectedly, the smallest instrument (Micro-NIRS) was the most precise for moisture and—together with portable NIRS—for IMF. According to Patel et al. (2021), this result could be due to data redundancy problems of the spectrometers with wider and more defined spectra. In pork, Wang et al. (2018a) and Wang et al. (2020b) found high correlations between NIR spectra and IMF, protein, and moisture content ($r_p \geq 0.86$) using portable dual-band Vis-NIR spectrometers in research labs and PLSR. In contrast, several studies reported low or unreliable NIRS predictability for IMF content in lambs at 24 to 28 h postmortem ($R^2_{cv} = 0.52$ to 0.55 or $R^2_{p} = 0.29$ to 0.54; Knight et al., 2019; Fowler et al., 2021b; Hitchman et al., 2021a; Lambe et al., 2021) and beef *longissimus thoracis* aged for 2 and 7 d ($R^2_{cv} = 0.08$ and 0.12, respectively; de Nadai Bonin et al., 2020), using portable Vis-NIR spectrometers (350 to 2,500 or 400 to 1,395 nm) and PLSR at commercial abattoirs. The lower NIRS predictability in these studies could be partly due to the narrower range of wavelengths and/or IMF content compared with those used in Dixit et al. (2020b). The latter could be due to differences among species, as lambs tend to have a narrower range of IMF than beef (Hoehne et al., 2012; Stewart et al., 2021; Hitchman et al., 2021b). Low NIRS predictability was also observed by Patel et al. (2021) for protein content in beef (coefficient of determination of calibration: $R^2_{c} = 0.61$, 0.51, and 0.62; $R^2_{p} = 0.46$, 0.23, and 0.43) using a portable VIS-NIR, a portable NIR, and a handheld micro-NIR spectrometer, respectively. These authors attributed the low R^2_{c} to the low variability of this chemical component in meat samples, whereas the low R^2_{p} were due to a greater proportion of farm/date variance, which was not reflected in the meat spectra.

Regarding NIRS ability to predict fatty acid (FA) composition, Prieto et al. (2018a) successfully estimated the content of FA groups and iodine value ($R^2_{p} = 0.81$ to 0.94), although lower predictability was reported for individual FA with low variability such as palmitic, stearic, and oleic FA ($R^2_{p} = 0.60$ to 0.70) in pork subcutaneous fat, using a portable NIRS device (350 to 2,500 nm) in a research abattoir and PLSR (Figure 6). Piao et al. (2018) found moderate NIRS predictability for monounsaturated FA (MUFA), oleic, and saturated FA (SFA) in beef intermuscular fat ($R^2_{p} = 0.69$, 0.64, and 0.67, respectively), using a 700 to 1,050 nm portable NIR spectrometer at meat markets and PLSR. When spectra were collected on intact lamb meat samples, accurate NIRS predictions were found

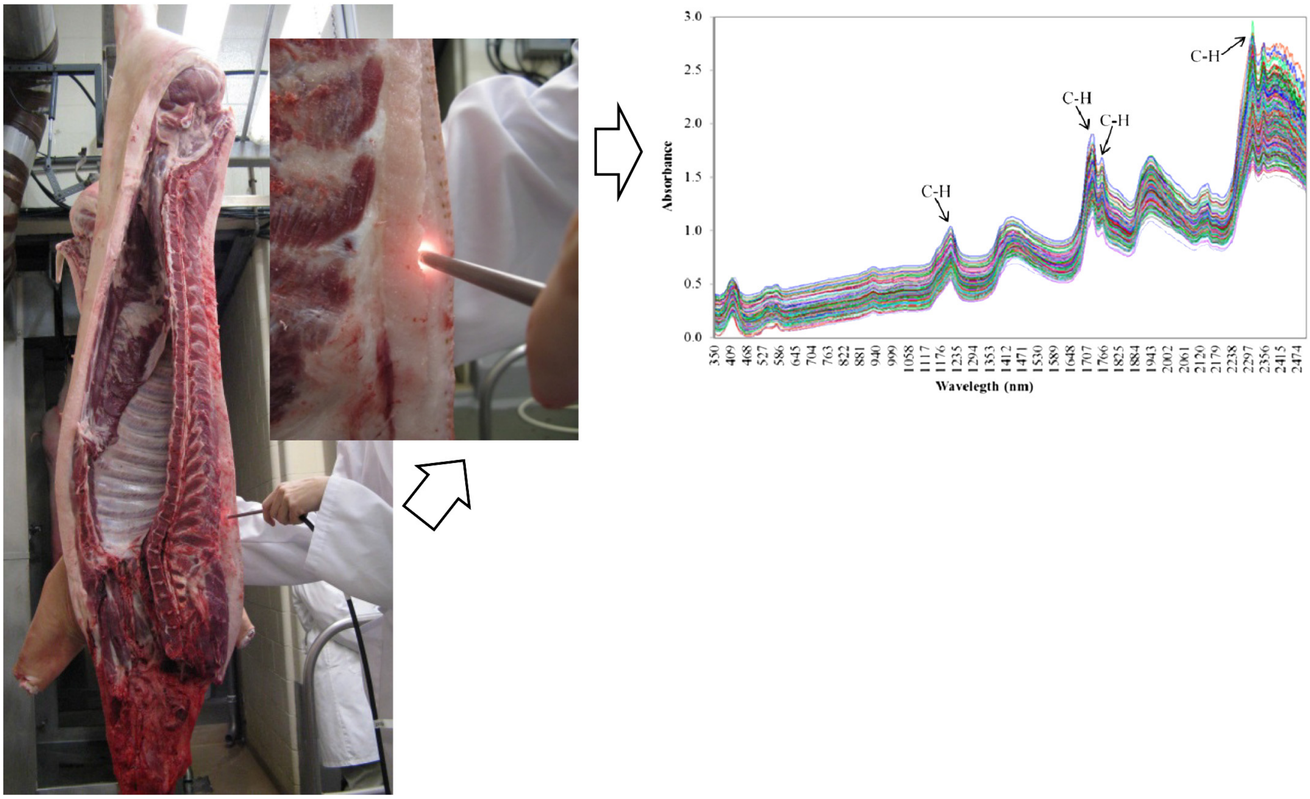

Figure 6. Collection of near-infrared spectra from the inner layer of pig carcass subcutaneous fat using a portable NIRS device (Prieto et al., 2018a). Source: Agriculture and Agri-Food Canada–Lacombe Research and Development Centre.

for SFA and polyunsaturated FA (R^2_{cv} = 0.84 and 0.94, respectively), and moderately accurate predictions were found for MUFA content (R^2_{cv} = 0.57), using a 350 to 2,500 nm portable spectrometer in a research abattoir and PLSR (Juárez et al., 2017). However, low NIRS predictability for individual and groups of FA (R^2_{cv} = 0.11 to 0.56) were found in intact lamb meat samples by Fiorentini et al. (2017), using a 350 to 2,500 nm portable instrument and PLSR. Apart from low variability, another limiting factor for FA prediction by NIRS is the similar absorption patterns of different FA due to similarities in chemical structure and functional groups (Prieto et al., 2017; Tao and Ngadi, 2018). This condition could generate complex relationships between the spectra and the response variables that are not capable of being predicted under a PLSR model. In fact, Barragán-Hernández et al. (2020) considerably improved NIRS predictability of individual and groups of FA in ground beef samples when support vector machine-learning (SVM) regression was applied (R^2_p = 0.74 to 0.99) compared with PLSR (R^2_p = 0.06 to 0.58). Therefore, regression based on SVM could be a novel alternative that manages to identify several vectors in hyperspace capable of constructing a generalizable prediction model for estimating FA profiles in beef with higher accuracy than conventional methods.

Portable and handheld NIR spectrometers have also been used recently to predict pH of intact meat samples. Dixit et al. (2020b) and Wang et al. (2018a) reported high NIRS predictability and correlation for pH in beef at a commercial pilot plant ($R^2_p \geq 0.84$) and pork at a research laboratory ($r_p \geq 0.81$), respectively. However, several studies reported low predictive ability ($R^2_{cv} \leq$ 0.29 or $R^2_p \leq 0.30$) in beef, pork, and lamb meat at research laboratories or commercial abattoirs (Fiorentini et al., 2017; Andersen et al., 2018; Patel et al., 2021; Savoia et al., 2021); this is likely due to narrower ranges in pH values compared with the 2 above-mentioned studies.

Furthermore, portable and handheld spectrometers have been used to predict color values (L^*, a^*, and b^*) of intact meat samples at laboratories and research or commercial abattoirs. Savoia et al. (2021) and Juárez et al. (2017) reported high L^* predictability in beef ($R^2_p \geq 0.80$) and lamb (R^2_{cv} = 0.93), respectively, whereas Wang et al. (2018a) reported high correlations between NIR spectra and L^* (r_p = 0.89 to 0.90), a^* (r_p = 0.88 to 0.94), and b^* (r_p = 0.90 to 0.95) in pork. In contrast, other studies reported low to moderate NIRS predictability for beef L^* ($R^2_{cv} = 0.33$ to 0.49 or $R^2_p = 0.42$ to 0.52), a^* ($R^2_{cv} = 0.07$ to 0.32 or $R^2_p = 0.52$ to 0.71), and b^* ($R^2_{cv} = 0.19$ to 0.39 or $R^2_p = 0.35$ to 0.63; Sahar et al., 2019; Patel et al., 2021; Savoia et al., 2021) as well as for pork L^* ($R^2_{cv} = 0.63$), a^* ($R^2_{cv} = 0.72$), and b^* color values ($R^2_{cv} = 0.65$; Furtado et al., 2019). These differences among studies for NIRS predictability of color values could be partly due to instrument variations.

In the last few years, WHC of intact meat has also been estimated using portable and handheld NIR spectrometers. NIRS poorly predicted purge loss ($R^2_p \leq 0.31$; Savoia et al., 2021) and cook loss in beef ($R^2_{cv} \leq 0.45$ or $R^2_p \leq 0.25$; Sahar et al., 2019; Patel et al., 2021; Savoia et al., 2021) and drip loss in pork ($R^2_{cv} \leq 0.12$; Andersen et al., 2018; Savoia et al., 2021). Nevertheless, a relatively high correlation between NIR spectra and cook loss in pork ($r_p = 0.77$) was found by Wang et al. (2020b), probably due to a wider variability (higher standard deviation) in cook loss from this study compared with that from the above-mentioned studies.

Recently, many studies have tested the prediction performance of portable and handheld Vis-NIR spectrometers at research or commercial abattoirs to predict Warner-Bratzler shear force (WBSF) values in meat from different species, as tenderness is a driver of consumer satisfaction. However, low NIRS predictability for WBSF values has been reported for both beef and lamb intact meat samples ($R^2_{cv} < 0.41$ or $R^2_p < 0.20$; Juárez et al., 2017; Knight et al., 2019; Cafferky et al., 2020; Savoia et al., 2021). Apart from the moderate to low repeatability and reproducibility reported for meat quality physical attributes such as shear force (Patel et al., 2021), the poor NIRS predictability for WBSF might be just because tenderness of cooked meat is not explained by compositional differences or vibrational properties of fresh meat provided by the NIR spectra. Similarly, Cafferky et al. (2020) reported unreliable predictions for taste panel tenderness scores in beef at 1 and 2 d postmortem using a portable NIR spectrometer at a commercial chilling room ($R^2_{cv} = 0.06$) and a laboratory ($R^2_{cv} = 0.13$), respectively, and for other sensory attributes such as juiciness, crumbliness, and beef flavor ($R^2_{cv} = 0.04$ to 0.41).

NIRS has also been used recently to estimate pork belly firmness. Lam et al. (2020) and Soladoye et al. (2018) successfully predicted belly firmness (subjective scoring: $R^2_p = 0.66$ to 0.84; belly flop angle: $R^2_p = 0.71$ to 0.91) when subcutaneous fat at the shoulder and lean and subcutaneous fat belly layers were scanned, respectively, using portable VIS-NIR spectrometers (350 to 2,500 nm) in cold rooms of a research abattoir and PLSR.

In recent years, NIRS technology along with machine learning techniques have become popular tools for authenticating meat products based on species, geographic origins, animal diet, and freshness in research laboratories or abattoirs. Yang et al. (2018) classified beef, pork, and mutton samples with 100% accuracy using SVM. Weng et al. (2020) used a portable NIR spectrometer and deep convolutional neural network (DCNN) to successfully identify beef adulterated with pork ($R^2_p = 0.94$). Revilla et al. (2020) correctly classified 84% of dry-cured beef samples of a Protected Geographic Indication quality label and 100% of non–Protected Geographic Indication, using a benchtop NIR spectrometer and artificial neural network. Barragán et al. (2021) correctly classified 75% to 100% of subcutaneous fat and intact meat samples from cattle fed barley or corn using a portable Vis-NIRS instrument and applying linear SVM. These authors confirmed the successful application of the SVM technique in studies with relatively small data sets while allowing an external validation. Finally, Moon et al. (2020) classified "fresh," "likely spoiled," and "spoiled" sirloin beef samples with 86% to 96% accuracy, using a portable Vis-NIR spectrometer and a convolutional neural network–based machine learning algorithm.

Hyperspectral imaging

By integrating spectroscopy and imaging techniques, imaging spectrometry, also known as HSI, is used to acquire 20 or more equally distributed contiguous spectral bands with ranges throughout both the visible and near infrared regions, resulting in a highly informative characterization of reflectance and emittance spectrum (Goetz, 2009). This advantage has led to the application of HSI to identify components and characterize their spatial distribution in a product, substance, tissue, or environment. The use of HSI for predicting chemical composition, technological attributes, and adulteration in meat has been previously reviewed (Xiong et al., 2014; Siche et al., 2016; Prieto et al., 2018b). Since the latter reviews, multiple studies using HSI to predict these attributes have emerged in beef, lamb, and pork.

Recent studies successfully predicted pH values in red meat using various statistical approaches. Using moveable benchtop HSI scanners, Craigie et al. (2017) and Dixit et al. (2020a) reported a relatively high HSI predictability for pH in lamb ($R^2_p = 0.71$) and in a combination of beef, lamb, and venison ($R^2_p = 0.75$–0.86), respectively, using PLSR. Nevertheless, Dixit et al. (2020a) and Yao et al. (2019) found higher predictability for pH using DCNN in beef/lamb/venison ($R^2_p = 0.89$) and support vector regression (SVR) in pork using a portable scanner ($R^2_p = 0.93$), respectively. The higher performance observed with SVR compared with PLSR models agrees with Thissen et al. (2004), who concluded that, for spectral applications, SVR is more robust and able to account for nonlinear effects from temperature changes. In addition, Craigie et al. (2017) included outliers in the model in an attempt to replicate industry application results, which could result in the lower performance compared with the other studies. These authors suggested continued calibration and validation to improve the robustness of the model. When comparing HSI line (550 to 1,700 nm) and snapshot (670 to 950 nm) scan systems using a robotic platform inline in a meat processing pilot plant to predict muscle pH in beef, the line scanner showed superior performance ($R^2_p =$ 0.89) to the HSI snapshot scanner ($R^2_p = 0.77$; Dixit et al., 2020b). Although HSI snapshot scanners exhibit faster image acquisition, HSI line scanning systems are able to provide better sample representation, explaining this difference in performance.

Similar to pH studies discussed earlier, DCNN models performed slightly better ($R^2_p = 0.89$) than PLSR ($R^2_p = 0.84$ to 0.88) for IMF proportion prediction, when performing a combined analysis of beef, lamb, and venison using a benchtop HSI scanner with a moving stage (Dixit et al., 2020a). Likewise, HSI line scanning ($R^2_p = 0.90$) outperformed snapshot scanning systems ($R^2_p = 0.72$) when predicting beef IMF content inline in a meat processing pilot plant (Dixit et al., 2020b). In pork, several studies revealed high HSI prediction performance for IMF content in loin ($R^2_p = 0.86$ to 0.96), using benchtop and pushbroom lab HSI systems and several prediction models (step-wise regression, PLSR, SVM, and back-propagation neural networks) (Huang et al., 2014; Ma et al., 2018; Kucha et al., 2021a). Aheto et al. (2020) used a pushbroom HSI system in the laboratory to estimate IMF content in pork bellies and reported relatively high predictability when a median spectral features model ($R^2_p = 0.81$) and a mean image feature model ($R^2_p =$ 0.73) were used. When using HSI to predict IMF proportion in *longissimus lumborum* from lambs, moderate accuracy ($R^2_p = 0.67$; Craigie et al., 2017) and high accuracy ($R^2_p = 0.92$) were observed using PLSR and progressive PLSR (which cumulatively included data chronologically and recalculated the model) models, respectively. The latter used a line scanning system with a moving stage in a lab setting and suggested that, for inline HSI systems, updating the models over time (particularly where lighting and environmental conditions cannot be carefully controlled) might be a useful strategy to improve future predictions. Velásquez et al. (2017) reported pushbroom lab HSI as a successful technology to classify beef based on the degree of marbling using the decision tree method (99.92%).

The HSI has also been applied to predict FA concentration. Craigie et al. (2017) predicted groups (SFA, MUFA and polyunsaturated FA) and individual FA content with moderate ($R^2_p = 0.53$ to 0.70) and low accuracy ($R^2_p = 0.00$ to 0.48), respectively, in lamb meat using PLSR. The low HSI performance was likely due to the inclusion of outliers in an attempt to replicate an industry application scenario. In contrast, Wang et al. (2020a) found high HSI predictability using a lab benchtop moving stage HSI system for palmitic ($R^2_p = 0.91$) and oleic FA content ($R^2_p = 0.88$) in lamb meat, when HSI spectra were combined with texture data (using gray-level co-occurrence matrix to extract textural features) and variable combination population analysis–iteratively retaining informative variables was applied to an SVM regression (for palmitic acid prediction) and a PLSR model (for oleic acid prediction). For specific FA in pork, using full wavelength spectral data and mean spectral features, a recent study showed prediction performance for myristic, palmitic, palmitoleic, stearic, oleic, and linoleic FA ranging from R^2_p 0.69 to R^2 0.84 (Kucha et al., 2021b).

In addition to fat variables, other meat chemical components have been estimated using HSI. Water content was successfully predicted using a lab-based benchtop HSI and MLR in lambs ($R^2_p = 0.92$; Pu et al., 2014). Although still relatively high, lower HSI predictability was reported for protein content in lambs using MLR or PLSR ($R^2_p = 0.80$ to 0.85; Pu et al., 2014) and in pork using back-propagation neural networks ($R^2_{cv} = 0.78$ to 0.83; Ma et al., 2019). The overall lower performance for predicting protein content could be due to the low range/variability of this component (Prieto et al., 2018b).

Regarding color in red meat, high predictability with benchtop lab HSI systems was reported for L^*, a^*, and b^* values in combined beef, lamb, and pork samples using MLR ($R^2_p = 0.97$, 0.84, and 0.82, respectively; Kamruzzaman et al., 2016b) and in beef using PLSR ($R^2 = 0.98$, 0.92, and 0.95, respectively; Yu et al., 2020). Metmyoglobin content is known to influence meat color stability, and many studies recently found high HSI predictability for different metmyoglobin content variables in lambs using benchtop lab HSI systems and different prediction approaches including

PLSR and least-squares support vector machines (LSSVM) ($R^2_p = 0.85$ and 0.91, respectively; Cheng et al., 2020), competitive adaptive reweighted sampling–LSSVM ($R^2_p = 0.81$ to 0.91; Yu et al., 2020), NIR-HSI data combined with generalized 2D correlation spectroscopy method ($R^2_p = 0.85$; Cheng et al., 2021), and competitive adaptive reweighted sampling–PLSR ($R^2_p = 0.77$; Yuan et al., 2020). Few studies have recently applied HSI to predict WHC in meat. Kamruzzaman et al. (2016a) predicted with high accuracy drip loss in beef, lamb, and pork together using a benchtop HSI in a lab environment and PLSR ($R^2_p = 0.92$) and SVM ($R^2_p = 0.94$).

Regarding the prediction of instrumental tenderness (WBSF) using a benchtop HSI system in a lab setting, Balage et al. (2018) reported low predictability in beef using a specific region of interest ($R^2_p = 0.06$ to 0.27) and PLSR. These authors concluded that HSI applied to a specific region of the sample does not accurately represent the tenderness of the whole sample. Nubiato et al. (2018) used a lab-based benchtop HSI to classify beef samples based on WBSF values and reported that 89.9% and 84.8% of samples were correctly classified using partial (928 to 1,413 nm) and full (928 to 2,524 nm) wavelength, respectively. When HSI systems were recently used inline in a meat processing pilot plant, Dixit et al. (2020b) reported a poor prediction performance using an HSI line ($R^2_p = 0.17$ to 0.36) and a snapshot scanner ($R^2_p = 0.13$ to 0.18) for WBSF value in beef aged for different aging periods. These authors suggested that the low performance could either be due to a lack of direct correlation between WBSF and spectral features or be due to the fact that all the muscles were not in rigor at the scanning time. Considering that the spectroscopic measurements were taken at 24 h postmortem and WBSF measurements were performed in aged meat, this might have limited the prediction performance of WBSF.

The detection of meat adulteration (i.e., with spoiled meat or other animal meats) has been successful using HSI. Recent studies have shown high HSI prediction performance of detecting proportions of adulterated meat (by mixing spoiled meat) in beef ($R^2_p = 0.94$; Zhao et al., 2019) and mutton ($R^2_p = 0.93$; Zhu et al., 2021) using benchtop systems in a lab setting and SVM. Minced lamb meat and beef adulteration with duck meat have been accurately predicted using a lab HSI system with moving stage and PLSR and principal component regression modeling methods ($R^2_p > 0.95$; Jiang et al., 2019; Zheng et al., 2019). Rady and Adedeji (2020) used a pushbroom HSI system in a laboratory and PLSR model to detect adulteration in minced meat for beef and pork, reporting a classification rate of 75%–100% and 100% for pure and adulterated samples, respectively.

Raman spectroscopy

Raman spectroscopy is a type of vibrational spectroscopy that uses light spectra between 200 and 1,800 nm (50,000 to 5,556 cm^{-1}) and is based on light scattering. When photons collide with molecules, they sometimes exchange energy, which is referred to as Raman scattering (Smith and Dent, 2005). Biomolecules such as amino acids, collagen, elastin, carotenoids, FA, and cholesterols contribute to Raman scattering in meat and fish, and Raman spectroscopy is used to obtain information regarding the concentration, structure, and interactions among these biomolecules (Damez and Clerjon, 2008; Yang and Ying, 2011; Czamara et al., 2015). There are several advantages of Raman spectroscopy over traditional techniques that have been used to assess meat quality traits. Raman spectroscopy is a nondestructive, low-cost, and highly sensitive technology that requires a small sample and short analysis time. Additionally, there is no solvent use or toxic waste involved, and the spectra of water do not interfere with those of other meat components (Motoyama, 2017; Pallone et al., 2018; Chen et al., 2020). However, one disadvantage of Raman spectroscopy is fluorescent background interference, especially in lean meats that contain fluorescing compounds, but algorithms have been recently developed to subtract fluorescent background (Wang et al., 2018b).

Raman spectroscopy has been widely used to predict chemical composition of meat (Yang and Ying, 2011; Troy et al., 2016). When scanning intact meat using lab benchtop instruments, Andersen et al. (2018) and Cama-Moncunill et al. (2020) found moderate predictability for IMF content from 4- to 5-d aged pork ($R^2_{cv} = 0.73$) and 2-d aged beef LTL ($R^2_{cv} = 0.64$), respectively, using PLSR. The latter indicated that contribution from non–readily identified bands probably not related to the variation of IMF might explain the modest spectral variance explained by the model. To date, there are not many studies applying handheld Raman spectrometers to predict chemical composition of intact meat. In this context, low Raman predictability was reported by Fowler et al. (2015a) for IMF and FA group content in lamb meat at a research laboratory ($R^2_{cv} = 0.01$ to 0.21). These authors hypothesized that the process of separating protein and lipid spectra might have reduced the ability to predict major FA composition, because removing all spectra that contained mixed lipid and protein signals might also have removed information on the phospholipids bound in membranes.

Furthermore, portable and handheld Raman spectrometers have been used in research laboratories to predict pH and color values of meat. Moderate predictions for ultimate pH were reported for intact pork ($R^2_{cv} = 0.52$ to 0.72; Andersen et al., 2018, 2021) and lamb meat ($R^2_{cv} = 0.59$; Fowler et al., 2015b), but predictions were lower for beef ($R^2 = 0.42$; Fowler et al., 2018). Fowler et al. (2018) indicated that a high loin purge (7%, probably due to a rapid pH decline) could have caused less Raman information present in spectra, resulting in poorer predictions of pH in meat. Additionally, Yang et al. (2020) reported high Raman predictability for pH and L^* at 0-d aged beef steaks ($R^2_{cv} = 0.99$ and 0.78, respectively), but these values declined steadily over a 21-d aging period, reaching a minimum R^2_{cv} of 0.04 for both attributes. Attempts to predict a^* and b^* were unsuccessful. Similarly, poor predictions were reported for L^* in lamb at 1 d and 5 d postmortem ($R^2_{cv} = 0.32$ and 0.22, respectively; Fowler et al., 2015b).

Raman spectroscopy has also been applied to estimate WHC. When scanning intact meat in a laboratory, moderate Raman predictability was found by Andersen et al. (2021) for drip loss ($R^2_{cv} = 0.56$ to 0.75). However, low predictability was reported for drip loss in pork ($R^2_{cv} = 0.49$; Andersen et al., 2018) and drip loss and cook loss in beef ($R^2_{cv} = 0.59$ and 0.49, respectively; Cama-Moncunill et al., 2020), using lab benchtop instruments. Cama-Moncunill et al. (2020) indicated the contribution from non–readily identified bands in the predictions that might not be related to the variation of physicochemical characteristics of the samples and the experimental design (drip and cook loss were measured on 2-d aged fresh and 14-d aged thawed muscle, respectively, whereas Raman spectra were collected on 2-d aged thawed muscle) as factors that could have jeopardized the accuracy of the predictions. Fowler et al. (2018) predicted with low accuracy purge loss in beef ($R^2 = 0.46$) using a handheld Raman spectrometer at the laboratory.

Discrepancies among recent studies have been found predicting instrumental tenderness by Raman spectroscopy in intact meat from different species. Using a lab benchtop spectrometer to predict WBSF values, Cama-Moncunill et al. (2020) found low accuracy in beef ($R^2_{cv} = 0.36$). These authors suggested that the low predictability could be a result of including signals unrelated to physical/chemical changes in their model because some bands in their plots were uninterpretable and only small spectral changes were observed between tender and tough meat. Chen et al. (2020) found high predictive ability for shear force in beef, as measured with a Meullenet–Owens razor shear probe, using a portable Raman spectrometer in a laboratory ($R^2_{p} = 0.81$). When handheld Raman spectrometers were used at the laboratory, Fowler et al. (2018) and Fowler et al. (2014) found unreliable Raman predictability for WBSF in beef ($R^2 = 0.11$) and lamb ($R^2_{cv} = 0.06$), respectively. Fowler et al. (2014) attributed the low performance to Raman measurements being taken on the thinnest side of the *longissimus lumborum* samples because, owing to the close proximity of 3 muscle surfaces, diffuse scattering might have increased, thereby preventing signal discrimination in deeper areas of the muscle. Additionally, these authors hypothesized that increasing the integration time from 3 s or increasing the total accumulation by including repetitions would improve the accuracy of prediction by reducing the signal to noise ratio. When Raman spectroscopy was used for classification purposes, Santos et al. (2018) correctly classified >67% and >85% of pork samples based on instrumental tenderness at 1 d postmortem in a commercial abattoir and at 15 d postmortem in a laboratory, respectively, using a portable Raman spectrometer and SVM.

When tenderness was evaluated by untrained consumers, high accuracy predictions were reported using a handheld Raman spectrometer in intact lamb meat ($R^2 = 0.99$; Fowler et al., 2021a). Additionally, Santos et al. (2018) correctly classified pork samples based on tenderness assessed by trained panelists at 1 d postmortem in a commercial abattoir (>69%) and at 15 d postmortem in a laboratory (>93%), using a portable Raman spectrometer and SVM. Overall, these results indicate that Raman spectroscopy might be a better predictor of sensory tenderness than shear force. This is likely due to sensory tenderness being associated with more than one biochemical characteristic, whereas the measurement of shear force does not take into account the contribution of water and fat content to the sensory perception of juiciness and the impact this has on the perception of tenderness (Perry et al., 2001).

Recent cases of meat adulteration, such as the report of horse DNA in 33% of frozen beef burgers (Laurence, 2013), have increased the use of Raman spectroscopy to discriminate meat based on species, feeding regimes, or cuts. Robert et al. (2021) discriminated among beef, venison, and lamb with over 80% accuracy using partial least square discriminant analysis (PLS-DA) and a benchtop spectrometer. Additionally, Logan et al. (2021) correctly classify beef fed long-term grain, short-term grain, grass, and a supplemented grass diet (96%, 85%, 83%, and 83%, respectively), using a handheld Raman spectrometer directly on the carcass subcutaneous fat and PLS-DA. Martin-Gomez et al. (2021) used a portable Raman spectrometer in a laboratory and a K-nearest neighbours algorithm to correctly classify 83.3% of dry-cured hams based on pork diet and 77.8% to 100% of dry-cured hams based on breed. Furthermore, Ostovar Pour et al. (2020) distinguished beef cuts (rump, Scotch fillet, round, chuck, tenderloin, and T-bone) with 84.4% accuracy, using a portable Raman spectrometer in a laboratory and principal component discriminant function analysis.

Conclusions

Sensing technologies are powerful tools for nondestructive assessment of carcass merit and meat and fat quality traits in livestock. However, equipment price and time required to scan or process the vast amount of information generated by these technologies have limited their use in industrial applications. Nevertheless, continuous efforts to evolve and refine instruments to achieve online prototypes capable of working safely at line speed have allowed the evolution of sensing technologies to successfully estimate not only total composition of the whole carcass but also the primal and retail cuts. In the last few years, the use of spectroscopic technologies that use portable and, particularly, handheld devices, in tandem with advanced machine learning algorithms, has increased, which has overcome some of the limitations and improved the feasibility of using these technologies for meat applications. However, most of the studies in the literature were primarily performed at laboratory scale or in pilot processing plants, and there was a lack of studies proving the robustness of models at processing plants. Therefore, further refinements in the devices, research on larger independent data sets, and the integration of machine learning approaches accounting for sources of variation might increase the commercial deployment of these sensing technologies in the meat industry.

Acknowledgments

The authors wish to thank the Organizing Committee of the 2021 Reciprocal Meat Conference for the opportunity to develop and present this review.

Literature Cited

Aalhus, J. L., Ó. López-Campos, N. Prieto, A. Rodas-González, M. E. R. Dugan, B. Uttaro, and M. Juárez. 2014. Review: Canadian beef grading—Opportunities to identify carcass and meat quality traits valued by consumers. Can. J. Anim. Sci. 94:545–556. https://doi.org/10.4141/cjas-2014-038.

Afonso, J., C. Guedes, V. Santos, R. Morais, J. Silva, A. Teixeira, and S. Silva. 2020. Utilization of bioelectrical impedance to predict intramuscular fat and physicochemical traits of the beef longissimus thoracis et lumborum muscle. Foods. 9:836. https://doi.org/10.3390/foods9060836.

Agarwal, U. P., and R. H. Atalla. 2010. Vibrational spectroscopy. In: C. Heitner, D. Dimmel, and J. Schmidt, editors, Lignin and lignans: advances in chemistry. 1st edition. CRC Press, Boca Raton, Florida. p. 103–136.

Aheto, J. H., X. Huang, X. Tian, Y. Ren, B. Ernest, E. A. Alenyorege, C. Dai, T. Hongyang, Z. Xiaorui, and P. Wang. 2020. Multi-sensor integration approach based on hyperspectral imaging and electronic nose for quantitation of fat and peroxide value of pork meat. Anal. Bioanal. Chem. 412:1169–1179. https://doi.org/10.1007/s00216-019-02345-5.

Alempijevic, A., T. Vidal-Calleja, R. Falque, P. Quin, E. Toohey, B. Walmsley, and M. McPhee. 2021. Lean meat yield estimation using a prototype 3D imaging approach. Meat Sci. 181:108470. https://doi.org/10.1016/j.meatsci.2021.108470.

An, J. S., J. H. Lee, M. H. Song, W. Yun, H. J. Oh, Y. J. Kim, J. S. Lee, H. B. Kim, and J. H. Cho. 2021. Predicting body compositions of live finishing pigs based on bioelectrical impedance analysis. J. Anim. Sci. Tech. 63:332–338. https://doi.org/10.5187/jast.2021.e31.

Andersen, P. V., N. K. Afseth, E. Gjerlaug-Enger, and J. P. Wold. 2021. Prediction of water holding capacity and pH in porcine longissimus lumborum using Raman spectroscopy. Meat Sci. 172:108357. https://doi.org/10.1016/j.meatsci.2020.108357.

Andersen, P. V., J. P. Wold, E. Gjerlaug-Enger, and E. Veiseth-Kent. 2018. Predicting post-mortem meat quality in porcine longissimus lumborum using Raman, near infrared and fluorescence spectroscopy. Meat Sci. 145:94–100. https://doi.org/10.1016/j.meatsci.2018.06.016.

Anderson, F., C. Payne, L. Pannier, D. W. Pethick, and G. E. Gardner. 2021. The potential for dual energy X-ray absorptiometry to predict lamb eating quality. Meat Sci. 181:108434. https://doi.org/10.1016/j.meatsci.2021.108434.

Andueza, D., A. Listrat, D. Durand, J. Normand, B. P. Mourot, and D. Gruffat. 2019. Prediction of beef meat fatty acid composition by visible-near-infrared spectroscopy was improved by preliminary freeze-drying. Meat Sci. 158:107910. https://doi.org/10.1016/j.meatsci.2019.107910.

Araújo, J. C., A. C. S. Lima, M. P. M. Nunes, M. A. P. Sousa, G. X. Serrão, E. C. Morais, L. C. C. Daher, and A. G. M. Silva. 2020. Relationships among carcass shape, tissue composition, primal cuts and meat quality traits in lambs: A PLS path modeling approach. Small Ruminant Res. 182:52–66. https://doi.org/10.1016/j.smallrumres.2019.106024.

Balage, J. M., J. M. Amigo, D. S. Antonelo, M. R. Mazon, and S. da Luz e Silva. 2018. Shear force analysis by core location in Longissimus steaks from Nellore cattle using hyperspectral images—A feasibility study. Meat Sci. 143:30–38. https://doi.org/10.1016/j.meatsci.2018.04.003.

Barragán, W., J. L. Aalhus, G. Penner, M. E. R. Dugan, M. Juárez, Ó. López-Campos, P. Vahmani, J. Segura, J. Angulo, and N. Prieto. 2021. Authentication of barley-finished beef using visible and near infrared spectroscopy (Vis-NIRS) and different discrimination approaches. Meat Sci. 172:108342. https://doi.org/10.1016/j.meatsci.2020.108342.

Barragán-Hernández, W., L. Mahecha-Ledesma, W. Burgos-Paz, M. Olivera-Angel, and J. Angulo-Arizala. 2020. Using near-infrared spectroscopy to determine intramuscular fat and fatty acids of beef applying different prediction approaches. J. Anim. Sci. 98:1–10. https://doi.org/10.1093/jas/skaa342.

Batista, A. C., V. Santos, J. Afonso, C. Guedes, J. Azevedo, A. Teixeira, and S. Silva. 2021. Evaluation of an image analysis approach to predicting primal cuts and lean in light lamb carcasses. Animals-Basel. 11:1368. https://doi.org/10.3390/ani11051368.

Berg, E. P., and M. J. Marchello. 1994. Bioelectrical impedance analysis for the prediction of fat-free mass in lambs and lamb carcasses. J. Anim. Sci. 72:322–329. https://doi.org/10.2527/1994.722322x.

Cafferky, J., T. Sweeney, P. Allen, A. Sahar, G. Downey, A. R. Cromie, and R. M. Hamill. 2020. Investigating the use of visible and near infrared spectroscopy to predict sensory and texture attributes of beef M.longissimus thoracis et lumborum. Meat Sci. 159:107915. https://doi.org/10.1016/j.meatsci.2019.107915.

Calnan, H., A. Williams, J. Peterse, S. Starling, J. Cook, S. Connaughton, and G. E. Gardner. 2021. A prototype rapid dual energy X-ray absorptiometry (DEXA) system can predict the CT composition of beef carcases. Meat Sci. 173:108397. https://doi.org/10.1016/j.meatsci.2020.108397.

Cama-Moncunill, R., J. Cafferky, C. Augier, T. Sweeney, P. Allen, A. Ferragina, C. Sullivan, A. Cromie, and R. M. J. M. s. Hamill. 2020. Prediction of Warner-Bratzler shear force, intramuscular fat, drip-loss and cook-loss in beef via Raman spectroscopy and chemometrics. Meat Sci. 167:108157. https://doi.org/10.1016/j.meatsci.2020.108157.

Chen, Q., Y. Zhang, Y. Guo, Y. Cheng, H. Qian, W. Yao, Y. Xie, and Y. Ozaki. 2020. Non-destructive prediction of texture of frozen/thaw raw beef by Raman spectroscopy. J. Food Eng. 266:109693. https://doi.org/10.1016/j.jfoodeng.2019.109693.

Cheng, L., G. Liu, J. He, G. Wan, J. Ban, R. Yuan, and N. Fan. 2021. Development of a novel quantitative function between spectral value and metmyoglobin content in Tan mutton. Food Chem. 342:128351. https://doi.org/10.1016/j.foodchem.2020.128351.

Cheng, L., G. Liu, J. He, G. Wan, C. Ma, J. Ban, and L. Ma. 2020. Non-destructive assessment of the myoglobin content of Tan sheep using hyperspectral imaging. Meat Sci. 167:107988. https://doi.org/10.1016/j.meatsci.2019.107988.

Choi, J. S., K. M. Kwon, Y. K. Lee, J. U. Joeng, K. O. Lee, S. K. Jin, Y. I. Choi, and J. J. Lee. 2018. Application of AutoFom III equipment for prediction of primal and commercial cut weight of Korean pig carcasses. Asian Austral. J. Anim. 31:1670–1676. https://doi.org/10.5713/ajas.18.0240.

Cisneros, F., M. Ellis, K. D. Miller, J. Novakofski, E. R. Wilson, and F. K. McKeith. 1996. Comparison of transverse and longitudinal real-time ultrasound scans for prediction of lean cut yields and fat-free lean content in live pigs. J. Anim. Sci. 74:2566–2576. https://doi.org/10.2527/1996.74112566x.

Connaughton, S. L., A. Williams, F. Anderson, K. R. Kelman, and G. E. Gardner. 2020a. Dual energy X-ray absorptiometry precisely and accurately predicts lamb carcass composition at abattoir chain speed across a range of phenotypic and genotypic variables. Animal. 14:2194–2202. https://doi.org/10.1017/S1751731120001019.

Connaughton, S. L., A. Williams, F. Anderson, K. R. Kelman, J. Peterse, and G. E. Gardner. 2020b. Dual energy X-ray absorptiometry predicts lamb carcass composition at abattoir chain speed with high repeatability across varying processing factors. Meat Sci. 181:108413. https://doi.org/10.1016/j.meatsci.2020.108413.

Craigie, C. R., P. L. Johnson, P. R. Shorten, A. Charteris, G. Maclennan, M. L. Tate, M. P. Agnew, K. R. Taukiri, A. D. Stuart, and M. M. Reis. 2017. Application of hyperspectral imaging to predict the pH, intramuscular fatty acid content and composition of lamb M. longissimus lumborum at 24 h post mortem. Meat Sci. 132:19–28. https://doi.org/10.1016/j.meatsci.2017.04.010.

Czamara, K., K. Majzner, M. Z. Pacia, K. Kochan, A. Kaczor, and M. Baranska. 2015. Raman spectroscopy of lipids: A review. J. Raman Spectrosc. 46:4–20. https://doi.org/10.1002/jrs.4607.

Damez, J. L., and S. Clerjon. 2008. Meat quality assessment using biophysical methods related to meat structure. Meat Sci. 80:132–149. https://doi.org/10.1016/j.meatsci.2008.05.039.

de Nadai Bonin, M., S. da Luz e Silva, L. Bünger, D. Ross, G. L. Dias Feijó, R. da Costa Gomes, F. Palma Rennó, M. H. de Almeida Santana, F. Marcondes de Rezende, L. C. Vinhas Ítavo, F. J. de Novais, L. M. A. Surita, M. de Nadai Bonin, M. W. Filgueira Pereira, and J. B. S. Ferraz. 2020. Predicting the shear value and intramuscular fat in meat from Nellore cattle using Vis-NIR spectroscopy. Meat Sci. 163:108077. https://doi.org/10.1016/j.meatsci.2020.108077.

Diaz-Almanza, S., R. Reyes-Villagrana, A. D. Alarcon-Rojo, M. Huerta-Jimenez, L. M. Carrillo-Lopez, C. Estepp, J. Urbina-Perez, and I. A. Garcia-Galicia. 2019. Time matters when ultrasonicating beef: The best time for tenderness is not the best for reducing microbial counts. J. Food Process Eng. 42:e13210. https://doi.org/10.1111/jfpe.13210.

Dixit, Y., M. Al-Sarayreh, C. R. Craigie, and M. M. Reis. 2020a. A global calibration model for prediction of intramuscular fat and pH in red meat using hyperspectral imaging. Meat Sci. 181:108405. https://doi.org/10.1016/j.meatsci.2020.108405.

Dixit, Y., M. P. Casado-Gavalda, R. Cama-Moncunill, X. Cama-Moncunill, M. Markiewicz-Keszycka, P. J. Cullen, and C. Sullivan. 2017. Developments and challenges in online NIR spectroscopy for meat processing. Compr. Rev. Food Sci. F. 16:1172–1187. https://doi.org/10.1111/1541-4337.12295.

Dixit, Y., S. Hitchman, T. M. Hicks, P. Lim, C. K. Wong, L. Holibar, K. C. Gordon, M. Loeffen, M. M. Farouk, C. R. Craigie, and M. M. Reis. 2020b. Non-invasive spectroscopic and imaging systems for prediction of beef quality in a meat processing pilot plant. Meat Sci. 181:108410. https://doi.org/10.1016/j.meatsci.2020.108410.

Esberg, J., M. Christensen, and T. Lauridsen. 2019. Frontmatec BCC-3 beef classification system study and installation in Australia beef industry [Final Report]. Meat and Livestock Australia, North Sydney, Australia.

European Commission. 2011. Commission implementing decision of 16 August 2011 amending Decision 2005/240/EC authorising methods for grading pig carcasses in Poland (notified under document C[2011]5745). Publications Office of the European

Union. https://op.europa.eu/en/publication-detail/-/publication/8bc3bcfb-91db-4398-91bc-37fae17f21cd. (Accessed 25 June 2021).

European Commission. 2019. Commission implementing decision (EU) 2019/252 of 11 February 2019 amending Decision 2005/240/EC authorising methods for grading pig carcasses in Poland (notified under document C[2019] 811). Publications Office of the European Union. https://beta.op.europa.eu/en/publication-detail/-/publication/5125377b-2f60-11e9-8d04-01aa75ed71a1/language-en/format-PDF/source-199045991. (Accessed 25 June 2021).

Fallavena, L. P., L. D. Ferreira Marczak, and G. D. Mercali. 2020. Ultrasound application for quality improvement of beef Biceps femoris physicochemical characteristics. LWT-Food Sci. Technol. 118:108817. https://doi.org/10.1016/j.lwt.2019.108817.

Fiorentini, G., C. A. Fugita, L. Bellomo, A. I. Negueruela, C. Sañudo, and M. M. Campo. 2017. NIR determination of meat quality characteristics at different lamb carcass points. *Congress Proceedings, 63rd International Congress of Meat Science & Technology*, Cork, Ireland, 13–18 August 2017.

Font-i-Furnols, M., and M. Gispert. 2009. Comparison of different devices for predicting the lean meat percentage of pig carcasses. Meat Sci. 83:443–446. https://doi.org/10.1016/j.meatsci.2009.06.018.

Font-i-Furnols, M., A. Brun, and M. Gispert. 2019. Intramuscular fat content in different muscles, locations, weights and genotype-sexes and its prediction in live pigs with computed tomography. Animal. 13:666–674. https://doi.org/10.1017/S1751731118002021.

Font-i-Furnols, M., M. Terré, A. Brun, M. Vidal, and A. Bach. 2021. Prediction of tissue composition of live dairy calves and carcasses by computed tomography. Livest. Sci. 243:104371. https://doi.org/10.1016/j.livsci.2020.104371.

Fowler, S. M., B. W. B. Holman, M. T. Newell, G. Refshauge, R. C. Hayes, and D. L. Hopkins. 2021a. Prediction of eating quality of lamb loin using Raman spectroscopic technologies. *Congress Proceedings, 33rd Biennial Conference of the Australian Association of Animal Sciences*, Perth, Australia, 1–3 February 2021.

Fowler, S. M., E. N. Ponnampalam, H. Schmidt, P. Wynn, and D. L. Hopkins. 2015a. Prediction of intramuscular fat content and major fatty acid groups of lamb M. longissimus lumborum using Raman spectroscopy. Meat Sci. 110:70–75. https://doi.org/10.1016/j.meatsci.2015.06.016.

Fowler, S. M., H. Schmidt, R. van de Ven, and D. L. Hopkins. 2018. Preliminary investigation of the use of Raman spectroscopy to predict meat and eating quality traits of beef loins. Meat Sci. 138:53–58. https://doi.org/10.1016/j.meatsci.2018.01.002.

Fowler, S. M., H. Schmidt, R. van de Ven, P. Wynn, and D. L. Hopkins. 2015b. Predicting meat quality traits of ovine m. semimembranosus, both fresh and following freezing and thawing, using a hand held Raman spectroscopic device. Meat Sci. 108:138–144. https://doi.org/10.1016/j.meatsci.2015.06.010.

Fowler, S. M., H. Schmidt, R. van de Ven, P. Wynn, and D. L. Hopkins. 2014. Raman spectroscopy compared against traditional predictors of shear force in lamb m. longissimus lumborum. Meat Sci. 98:652–656. https://doi.org/10.1016/j.meatsci.2014.06.042.

Fowler, S. M., D. Wheeler, S. Morris, S. I. Mortimer, and D. L. Hopkins. 2021b. Partial least squares and machine learning for the prediction of intramuscular fat content of lamb loin. Meat Sci. 177:108505. https://doi.org/10.1016/j.meatsci.2021.108505.

Froehlich, E. J., J. G. Carlberg, and C. E. Ward. 2009. Willingness-to-pay for fresh brand name beef. Can. J. Agr. Econ. 57:119–137. https://doi.org/10.1111/j.1744-7976.2008.01141.x.

Fukuda, O., I. Ahmed, and D. Hashimoto. 2017. Estimation of marbling score in live beef cattle using Bayesian network. SICE Journal of Control, Measurement, and System Integration. 10:297–302. https://doi.org/10.9746/jcmsi.10.297.

Furtado, E. J. G., A. M. Bridi, D. F. Barbin, C. C. P. Barata, L. M. Peres, A. P. A. d. C. Barbon, N. Andreo, B. d. L. Giangareli, D. K. Terto, and J. P. Batista. 2019. Prediction of pH and color in pork meat using VIS-NIR Near-infrared Spectroscopy (NIRS). Food Sci. Tech.-Brazil. 39:88–92. https://doi.org/10.1590/fst.27417.

Gardner, G. E., F. Anderson, C. Smith, and A. Williams. 2021. Using dual energy X-ray absorptiometry to estimate commercial cut weights at abattoir chain-speed. Meat Sci. 173:108400. https://doi.org/10.1016/j.meatsci.2020.108400.

Gardner, G. E., S. Starling, J. Charnley, J. Hocking-Edwards, J. Peterse, and A. Williams. 2018. Calibration of an on-line dual energy X-ray absorptiometer for estimating carcase composition in lamb at abattoir chain-speed. Meat Sci. 144:91–99. https://doi.org/10.1016/j.meatsci.2018.06.020.

Geraldo, A. T., A. Bartholazzi Junior, C. M. Gomes David, A. C. Barros de Freitas, F. Antunes, M. A. Silva Rua, W. H. Ortiz Vega, J. Gazzoni Jardim, L. de Macêdo Mello, T. da Silva Correa, R. Travassos Beltrame, R. L. Dias da Costa, and C. R. Quirino. 2021. Body tissue development of Santa Inês breed sheep using computed tomography. Anim. Prod. Sci. 61:191–200. https://doi.org/doi.org/10.1071/AN20084.

Goetz, A. F. H. 2009. Three decades of hyperspectral remote sensing of the Earth: A personal view. Remote Sens. Environ. 113: S5–S16. https://doi.org/10.1016/j.rse.2007.12.014.

González, L. A., I. Kyriazakis, and L. O. Tedeschi. 2018. Review: precision nutrition of ruminants: Approaches, challenges and potential gains. Animal. 12:s246–s261. https://doi.org/10.1017/S1751731118002288.

Grunert, K. G., L. Bredahl, and K. Brunsø. 2004. Consumer perception of meat quality and implications for product development in the meat sector—A review. Meat Sci. 66:259–272. https://doi.org/10.1016/s0309-1740(03)00130-x.

Gundersen, H. J. G., T. F. Bendtsen, L. Korbo, N. Marcussen, A. Møller, K. Nielsen, J. R. Nyengaard, B. Pakkenberg, F. B. Sørensen, A. Vesterby, and M. J. West. 1988. Some new, simple and efficient stereological methods and their use in pathological research and diagnosis. APMIS. 96:379–394. https://doi.org/10.1111/j.1699-0463.1988.tb05320.x.

Hassoun, A., M. Guðjónsdóttir, M. A. Prieto, P. Garcia-Oliveira, J. Simal-Gandara, F. Marini, F. Di Donato, A. A. D'Archivio, and A. Biancolillo. 2020. Application of novel techniques for monitoring quality changes in meat and fish products during traditional processing processes: Reconciling novelty and tradition. Processes. 8:988. https://doi.org/10.3390/pr8080988.

Hitchman, S., P. Johnson, W. Bain, C. R. Craigie, and M. M. Reis. 2021a. Short communication: long term performance of near infrared spectroscopy to predict intramuscular fat content in New Zealand lamb. Meat Sci. 181:108376. https://doi.org/10.1016/j.meatsci.2020.108376.

Hitchman, S., M. P. F. Loeffen, M. M. Reis, and C. R. Craigie. 2021b. Robustness of hyperspectral imaging and PLSR model predictions of intramuscular fat in lamb M. longissimus lumborum across several flocks and years. Meat Sci. 179:108492. https://doi.org/10.1016/j.meatsci.2021.108492.

Hoehne, A., G. Nuernberg, C. Kuehn, and K. Nuernberg. 2012. Relationships between intramuscular fat content, selected carcass traits, and fatty acid profile in bulls using a F2-population. Meat Sci. 90:629–635. https://doi.org/10.1016/j.meatsci.2011.10.005.

Huang, H., L. Liu, M. O. Ngadi, C. Gariépy, and S. O. Prasher. 2014. Near-infrared spectral image analysis of pork marbling based on Gabor filter and wide line detector techniques. Appl. Spectrosc. 68:332–339. https://doi.org/10.1366/13-07242.

Huh, S., H. J. Kim, S. Lee, J. Cho, A. Jang, and J. Bae. 2021. Utilization of electrical impedance spectroscopy and image classification for non-invasive early assessment of meat freshness. Sensors-Basel. 21:1001. https://doi.org/10.3390/s21031001.

Janiszewski, P., K. Borzuta, D. Lisiak, E. Grze kowiak, and D. Stanisławski. 2019. Prediction of primal cuts by using an automatic ultrasonic device as a new method for estimating a pig-carcass slaughter and commercial value. Anim. Prod. Sci. 59:1183–1189. https://doi.org/10.1071/an15625.

Jayasooriya, S. D., B. R. Bhandari, P. Torley, and B. R. D'Arcy. 2004. Effect of high power ultrasound waves on properties of meat: A review. Int. J. Food Prop. 7:301–319. https://doi.org/10.1081/jfp-120030039.

Jiang, H., W. Wang, H. Zhuang, S.-C. Yoon, Y. Yang, and X. Zhao. 2019. Hyperspectral imaging for a rapid detection and visualization of duck meat adulteration in beef. Food Anal. Method. 12:2205–2215. https://doi.org/10.1007/s12161-019-01577-6.

Juárez, M., A. Horcada, N. Prieto, J. C. Roberts, M. E. R. Dugan, O. López-Campos, B. Uttaro, I. L. Larsen, S. Hosford, J. Galbraith, and J. L. Aalhus. 2017. Guaranteeing Canadian lamb meat quality using near-infrared spectroscopy on intact rack. Can. J. Anim. Sci. 98:390–393. https://doi.org/10.1139/cjas-2017-0106.

Kamruzzaman, M., Y. Makino, and S. Oshita. 2016a. Hyperspectral imaging for real-time monitoring of water holding capacity in red meat. LWT-Food Sci. Technol. 66:685–691. https://doi.org/10.1016/j.lwt.2015.11.021.

Kamruzzaman, M., Y. Makino, and S. Oshita. 2016b. Online monitoring of red meat color using hyperspectral imaging. Meat Sci. 116:110–117. https://doi.org/10.1016/j.meatsci.2016.02.004.

Kanoun, O. 2018. Impedance spectroscopy advances and future trends: a comprehensive review. In: O. Kanoun, editor, Impedance spectroscopy: Advanced applications: battery research, bioimpedance, system design. De Gruyter, Chemnitz, Germany. p. 1–21. https://doi.org/10.1515/9783110558920-001.

Kipper, M., M. Marcoux, I. Andretta, and C. Pomar. 2019. Assessing the accuracy of measurements obtained by dual-energy X-ray absorptiometry on pig carcasses and primal cuts. Meat Sci. 148:79–87. https://doi.org/10.1016/j.meatsci.2018.10.005.

Knight, M. I., N. Linden, E. N. Ponnampalam, M. G. Kerr, W. G. Brown, D. L. Hopkins, S. Baud, A. J. Ball, C. Borggaard, and I. Wesley. 2019. Development of VISNIR predictive regression models for ultimate pH, meat tenderness (shear force) and intramuscular fat content of Australian lamb. Meat Sci. 155:102–108. https://doi.org/10.1016/j.meatsci.2019.05.009.

Kress, K., J. Hartung, J. Jasny, V. Stefanski, and U. Weiler. 2020. Carcass characteristics and primal pork cuts of gilts, boars, immunocastrates and barrows using AutoFOM III data of a commercial abattoir. Animals-Basel. 10:1912. https://doi.org/10.3390/ani10101912.

Kucha, C. T., L. Liu, M. Ngadi, and C. Gariépy. 2021a. Anisotropic effect on the predictability of intramuscular fat content in pork by hyperspectral imaging and chemometrics. Meat Sci. 176:108458. https://doi.org/10.1016/j.meatsci.2021.108458.

Kucha, C. T., L. Liu, M. Ngadi, and C. Gariépy. 2021b. Assessment of intramuscular fat quality in pork using hyperspectral imaging. Food Eng. Rev. 13:274–289. https://doi.org/10.1007/s12393-020-09246-9.

Kutsanedzie, F. Y. H., Z. Guo, and Q. Chen. 2019. Advances in nondestructive methods for meat quality and safety monitoring. Food Rev. Int. 35:536–562. https://doi.org/10.1080/87559129.2019.1584814.

Lam, S., O. P. Soladoye, N. Prieto, B. Uttaro, J. L. Aalhus, I. Larsen, P. Shand, C. Gariépy, M. Juárez, and F. Miglior. 2020. Performance of near-infrared spectroscopy in pork shoulder as a predictor for pork belly softness. Can. J. Anim. Sci. 101:386–389. https://doi.org/10.1139/cjas-2020-0049.

Lambe, N. R., N. Clelland, J. Draper, E. M. Smith, J. Yates, and L. Bunger. 2021. Prediction of intramuscular fat in lamb by visible and near-infrared spectroscopy in an abattoir environment. Meat Sci. 171:108286. https://doi.org/10.1016/j.meatsci.2020.108286.

Laurence, F. 2013. Horsemeat scandal: the essential guide. The Guardian. https://www.theguardian.com/uk/2013/feb/15/horsemeat-scandal-the-essential-guide (Accessed 29 April 2021).

Le Cozler, Y., C. Allain, A. Caillot, J. M. Delouard, L. Delattre, T. Luginbuhl, and P. Faverdin. 2019a. High-precision scanning system for complete 3D cow body shape imaging and analysis of morphological traits. Comput. Electron. Agr. 157:447–453. https://doi.org/10.1016/j.compag.2019.01.019.

Le Cozler, Y., C. Allain, C. Xavier, L. Depuille, A. Caillot, J. M. Delouard, L. Delattre, T. Luginbuhl, and P. Faverdin. 2019b. Volume and surface area of Holstein dairy cows calculated from complete 3D shapes acquired using a high-precision scanning system: Interest for body weight estimation. Comput. Electron. Agr. 165:104977. https://doi.org/doi.org/10.1016/j.compag.2019.104977.

Logan, B. G., D. L. Hopkins, L. M. Schmidtke, and S. M. Fowler. 2021. Authenticating common Australian beef production systems using Raman spectroscopy. Food Control. 121:107652. https://doi.org/10.1016/j.foodcont.2020.107652.

Lohumi, S., C. Wakholi, J. H. Baek, B. D. Kim, S. J. Kang, H. S. Kim, Y. K. Yun, W. Y. Lee, S. H. Yoon, and B.-K. Cho. 2018. Nondestructive estimation of lean meat yield of South Korean pig carcasses using machine vision technique.

Korean J. Food Sci. Anim. Resour. 38:1109–1119. https://doi.org/10.5851/kosfa.2018.e44.

López-Campos, Ó., N. Prieto, M. Juárez, and J. L. Aalhus. 2019. New technologies available for livestock carcass classification and grading. CAB Reviews. 14:1. https://doi.org/10.1079/pavsnnr201914018.

López-Campos, Ó., J. C. Roberts, I. L. Larsen, N. Prieto, M. Juárez, M. E. R. Dugan, and J. L. Aalhus. 2018. Rapid and non-destructive determination of lean fat and bone content in beef using dual energy X-ray absorptiometry. Meat Sci. 146:140–146. https://doi.org/10.1016/j.meatsci.2018.07.009.

Lucas, D., A. Brun, M. Gispert, A. Carabús, J. Soler, J. Tibau, and M. Font-i-Furnols. 2017. Relationship between pig carcass characteristics measured in live pigs or carcasses with Piglog, Fat-o-Meat'er and computed tomography. Livest. Sci. 197:88–95. https://doi.org/10.1016/j.livsci.2017.01.010.

Ma, J., H. Pu, and D.-W. Sun. 2018. Predicting intramuscular fat content variations in boiled pork muscles by hyperspectral imaging using a novel spectral pre-processing technique. LWT-Food Sci. Technol. 94:119–128. https://doi.org/10.1016/j.lwt.2018.04.030.

Ma, J., D. Sun, H. Pu, Q. Wei, and X. Wang. 2019. Protein content evaluation of processed pork meats based on a novel single shot (snapshot) hyperspectral imaging sensor. J. Food Eng. 240:207–213. https://doi.org/10.1016/j.jfoodeng.2018.07.032.

Martin-Gomez, A., N. Arroyo-Manzanares, M. Garcia-Nicolas, A. I. Lopez-Lorente, S. Cardenas, I. Lopez-Garcia, P. Vinas, M. Hernandez-Cordoba, and L. Arce. 2021. Portable Raman spectrometer as a screening tool for characterization of Iberian dry-cured ham. Foods. 10:1177. https://doi.org/10.3390/foods10061177.

Masoumi, M., M. Marcoux, L. Maignel, and C. Pomar. 2021. Weight prediction of pork cuts and tissue composition using spectral graph wavelet. J. Food Eng. 299:110501. https://doi.org/10.1016/j.jfoodeng.2021.110501.

Meyerding, S. G. H., M. Gentz, B. Altmann, and L. Meier-Dinkel. 2018. Beef quality labels: a combination of sensory acceptance test, stated willingness to pay, and choice-based conjoint analysis. Appetite. 127:324–333. https://doi.org/10.1016/j.appet.2018.05.008.

Miller, G. A., J. J. Hyslop, D. Barclay, A. Edwards, W. Thomson, and C.-A. Duthie. 2019. Using 3D imaging and machine learning to predict liveweight and carcass characteristics of live finishing beef cattle. Front. Sustain. Food Syst. 3. https://doi.org/10.3389/fsufs.2019.00030.

Moon, E. J., Y. Kim, Y. Xu, Y. Na, A. J. Giaccia, and J. H. Lee. 2020. Evaluation of salmon, tuna, and beef freshness using a portable spectrometer. Sensors. 20:4299. https://doi.org/10.3390/s20154299.

Moro, A. B., D. B. Galvani, Y. R. Montanholi, P. Bertemes-Filho, R. S. Venturini, A. A. Martins, L. P. da Silva, and C. C. Pires. 2020. Assessing the composition of the soft tissue in lamb carcasses with bioimpedance and accessory measures. Meat Sci. 169:108192. https://doi.org/10.1016/j.meatsci.2020.108192.

Moro, A. B., C. C. Pires, L. P. da Silva, A. M. Menegon, R. S. Venturini, A. A. Martins, R. O. Mello, and D. B. Galvani. 2019. Prediction of physical characteristics of the lamb carcass using in vivo bioimpedance analysis. Animal. 13:1744–1749. https://doi.org/10.1017/S1751731118003178.

Motoyama, M. 2017. Raman spectroscopy for meat quality and safety assessment. In: A. Bekhit, editor, Advances in meat processing technology. CRC Press, Boca Raton, FL. p. 269–298.

Narsaiah, K., A. K. Biswas, and P. K. Mandal. 2019. Nondestructive methods for carcass and meat quality evaluation. In: A. K. Biswas, and P. K. Mandal, editors, Meat quality analysis: Advanced evaluation methods, techniques, and technologies. Elsevier, Amsterdam. p. 37–49.

Nubiato, K. E. Z., M. R. Mazon, D. S. Antonelo, C. R. Calkins, G. K. Naganathan, J. Subbiah, and S. da Luz e Silva. 2018. A bench-top hyperspectral imaging system to classify beef from Nellore cattle based on tenderness. Infrared Phys. Techn. 89:247–254. https://doi.org/10.1016/j.infrared.2018.01.005.

Olsen, E. V., L. B. Christensen, and D. B. Nielsen. 2017. A review of computed tomography and manual dissection for calibration of devices for pig carcass classification—Evaluation of uncertainty. Meat Sci. 123:35–44. https://doi.org/10.1016/j.meatsci.2016.08.013.

Ostovar Pour, S., S. M. Fowler, D. L. Hopkins, P. Torley, H. Gill, and E. W. Blanch. 2020. Differentiating various beef cuts using spatially offset Raman spectroscopy. J. Raman Spectrosc. 51:711–716. https://doi.org/10.1002/jrs.5830.

Pallone, J. A. L., E. T. d. S. Caramês, and P. D. Alamar. 2018. Green analytical chemistry applied in food analysis: Alternative techniques. Curr. Opin. Food Sci. 22:115–121. https://doi.org/10.1016/j.cofs.2018.01.009.

Pan, X., J. Zhu, W. Tai, and Y. Fu. 2021. An automated method to quantify the composition of live pigs based on computed tomography segmentation using deep neural networks. Comput. Electron. Agr. 183:105987. https://doi.org/10.1016/j.compag.2021.105987.

Park, B., A. D. Whittaker, R. K. Miller, and D. E. Bray. 1994. Measuring intramuscular fat in beef with ultrasonic frequency analysis. J. Anim. Sci. 72:117–125. https://doi.org/10.2527/1994.721117x.

Patel, N., H. Toledo-Alvarado, and G. Bittante. 2021. Performance of different portable and hand-held near-infrared spectrometers for predicting beef composition and quality characteristics in the abattoir without meat sampling. Meat Sci. 178:108518. https://doi.org/10.1016/j.meatsci.2021.108518.

Pathak, V., V. P. Singh, and Y. Sanjay. 2011. Ultrasound as a modern tool for carcass evaluation and meat processing: A review. International Journal of Meat Science. 1:83–92. https://doi.org/10.3923/ijmeat.2011.83.92.

Peña-González, E. M., A. D. Alarcón-Rojo, A. Rentería, I. García, E. Santellano, A. Quintero, and L. Luna. 2017. Quality and sensory profile of ultrasound-treated beef. Ital. J. Food Sci. 29:463–475. https://doi.org/10.14674/1120-1770/ijfs.v604.

Perry, D., J. M. Thompson, I. H. Hwang, A. Butchers, and A. F. Egan. 2001. Relationship between objective measurements and taste panel assessment of beef quality. Aust. J. Exp. Agr. 41:981–989. https://doi.org/10.1071/EA00023.

Piao, S., T. Okura, and M. Irie. 2018. On-site evaluation of Wagyu beef carcasses based on the monounsaturated, oleic, and saturated fatty acid composition using a handheld fiber-optic near-infrared spectrometer. Meat Sci. 137:258–264. https://doi.org/10.1016/j.meatsci.2017.11.032.

Polkinghorne, R. J., and J. M. Thompson. 2010. Meat standards and grading: A world view. Meat Sci. 86:227–235. https://doi.org/10.1016/j.meatsci.2010.05.010.

Prieto, N., M. E. R. Dugan, M. Juárez, Ó. López-Campos, R. T. Zijlstra, J. L. Aalhus, and J. Plaizier. 2018a. Using portable near-infrared spectroscopy to predict pig subcutaneous fat composition and iodine value. Can. J. Anim. Sci. 98:221–229. https://doi.org/10.1139/cjas-2017-0033.

Prieto, N., E. Osika, J. L. Aalhus, O. Lopez-Campos, M. Juarez, and O. Pawluczyk. 2018b. Application of hyperspectral imaging on meat and meat products. CAB Reviews. 13:1–11. https://doi.org/10.1079/pavsnnr201813042.

Prieto, N., O. Pawluczyk, M. E. R. Dugan, and J. L. Aalhus. 2017. A review of the principles and applications of near-infrared spectroscopy to characterize meat, fat, and meat products. Appl. Spectrosc. 71:1403–1426. https://doi.org/10.1177/0003702817709299.

Prieto, N., R. Roehe, P. Lavin, G. Batten, and S. Andres. 2009. Application of near infrared reflectance spectroscopy to predict meat and meat products quality: A review. Meat Sci. 83:175–186. https://doi.org/10.1016/j.meatsci.2009.04.016.

Pu, H., D.-W. Sun, J. Ma, D. Liu, and M. Kamruzzaman. 2014. Hierarchical variable selection for predicting chemical constituents in lamb meats using hyperspectral imaging. J. Food Eng. 143:44–52. https://doi.org/10.1016/j.jfoodeng.2014.06.025.

Rady, A., and A. A. Adedeji. 2020. Application of hyperspectral imaging and machine learning methods to detect and quantify adulterants in minced meats. Food Anal. Method. 13:970–981. https://doi.org/10.1007/s12161-020-01719-1.

Remus, A., L. Hauschild, S. Methot, and C. Pomar. 2020. Precision livestock farming: real-time estimation of daily protein deposition in growing-finishing pigs. Animal. 14:s360–s370. https://doi.org/10.1017/S1751731120001469.

Revilla, I., A. M.Vivar-Quintana, M. I. González-Martín, M. Hernández-Jiménez, I. Martínez-Martín, and P. Hernández-Ramos. 2020. NIR spectroscopy for discriminating and predicting the sensory profile of dry-cured beef "Cecina." Sensors. 20:6892. https://doi.org/10.3390/s20236892.

Ripoll, G., M. Joy, J. Alvarez-Rodriguez, A. Sanz, and A. Teixeira. 2009. Estimation of light lamb carcass composition by in vivo real-time ultrasonography at four anatomical locations. J. Anim. Sci. 87:1455–1463. https://doi.org/10.2527/jas.2008-1285.

Robert, C., S. J. Fraser-Miller, W. T. Jessep, W. E. Bain, T. M. Hicks, J. F. Ward, C. R. Craigie, M. Loeffen, and K. C. Gordon. 2021. Rapid discrimination of intact beef, venison and lamb meat using Raman spectroscopy. Food Chem. 343:128441. https://doi.org/10.1016/j.foodchem.2020.128441.

Sahar, A., P. Allen, T. Sweeney, J. Cafferky, G. Downey, A. Cromie, and R. M. Hamill. 2019. Online prediction of physico-chemical quality attributes of beef using visible-near-infrared spectroscopy and chemometrics. Foods. 8:525. https://doi.org/10.3390/foods8110525.

Samperio, E., I. Lidón, R. Rebollar, M. Castejón-Limas, and C. Álvarez-Aparicio. 2021. Lambs' live weight estimation using 3D images. Animal. 15:100212. https://doi.org/10.1016/j.animal.2021.100212.

Santos, C. C., J. Zhao, X. Dong, S. M. Lonergan, E. Huff-Lonergan, A. Outhouse, K. B. Carlson, K. J. Prusa, C. A. Fedler, C. Yu, S. D. Shackelford, D. A. King, and T. L. Wheeler. 2018. Predicting aged pork quality using a portable Raman device. Meat Sci. 145:79–85. https://doi.org/10.1016/j.meatsci.2018.05.021.

Savoia, S., A. Albera, A. Brugiapaglia, L. Di Stasio, A. Cecchinato, and G. Bittante. 2021. Prediction of meat quality traits in the abattoir using portable near-infrared spectrometers: heritability of predicted traits and genetic correlations with laboratory-measured traits. J. Anim. Sci. Biotechno. 12:1. https://doi.org/10.1186/s40104-021-00555-5.

Segura, J., J. L. Aalhus, N. Prieto, I. L. Larsen, M. Juárez, and Ó. López-Campos. 2021. Carcass and primal composition predictions using camera vision systems (CVS) and dual-energy X-ray absorptiometry (DXA) technologies on mature cows. Foods. 10:1118. https://doi.org/10.3390/foods10051118.

Siche, R., R. Vejarano, V. Aredo, L. Velasquez, E. Saldana, and R. Quevedo. 2016. Evaluation of food quality and safety with hyperspectral imaging (HSI). Food Eng. Rev. 8:306–322. https://doi.org/10.1007/s12393-015-9137-8.

Smith, E., and G. Dent. 2005. Modern raman spectroscopy: a practical approach. John Wiley & Sons, Ltd, Chichester, West Sussex, England.

Soladoye, O. P., N. Prieto, O. Lopez-Campos, J. L. Aalhus, B. Uttaro, J. C. Roberts, I. Larsen, P. Shand, C. Gariepy, and M. Juarez. 2018. Potential of near infrared (NIR) spectroscopy and dual energy X-ray absorptiometry (DXA) in predicting pork belly softness. Meat Sci. 142:1–4. https://doi.org/10.1016/j.meatsci.2018.03.025.

Sousa dos Santos, L., P. H. Reis Furtado Campos, W. Cândido da Silva, A. M. Veira, A. Z. Fraga, R. P. Caetano, and L. Hauschild. 2021. Corrigendum to: Performance and carcass composition of pigs from two sire lines are affected differently by ambient temperature. Anim. Prod. Sci. 61:620–620. https://doi.org/10.1071/AN20078_CO.

Stewart, S. M., T. Lauridsen, H. Toft, D. W. Pethick, G. E. Gardner, P. McGilchrist, and M. Christensen. 2021. Objective grading of eye muscle area, intramuscular fat and marbling in Australian beef and lamb. Meat Sci. 181:108358. https://doi.org/10.1016/j.meatsci.2020.108358 (in press).

Swantek, P. M., J. D. Crenshaw, M. J. Marchello, and H. C. Lukaski. 1992. Bioelectrical impedance: a nondestructive method to determine fat-free mass of live market swine and pork carcasses J. Anim. Sci. 70:169–177. https://doi.org/10.2527/1992.701169x.

Szyndler-N dza, M., R. Eckert, and T. Blicharski. 2016. Prediction of carcass meat percentage in young pigs using linear regression models and artificial neural networks. Ann. Anim. Sci. 16:275–286. https://doi.org/10.1515/aoas-2015-0057.

Tait, R. G. J. 2016. Ultrasound use for body composition and carcass quality assessment in cattle and lambs. Vet. Clin. N. Am.-Food A. 32:207–218. https://doi.org/10.1016/j.cvfa.2015.09.007.

Tao, F., and M. Ngadi. 2018. Recent advances in rapid and nondestructive determination of fat content and fatty acids composition of muscle foods. Crit. Rev. Food Sci. 58:1565–1593. https://doi.org/10.1080/10408398.2016.1261332.

Theriault, M., C. Pomar, and F. W. Castonguay. 2009. Accuracy of real-time ultrasound measurements of total tissue, fat, and muscle depths at different measuring sites in lamb. J. Anim. Sci. 87:1801–1813. https://doi.org/10.2527/jas.2008-1002.

Thissen, U., M. Pepers, B. Üstün, W. J. Melssen, and L. M. C. Buydens. 2004. Comparing support vector machines to PLS for spectral regression applications. Chemometr. Intell. Lab. 73:169–179. https://doi.org/10.1016/j.chemolab.2004.01.002.

Tomasević, I., V. Tomović, B. Milovanović, J. Lorenzo, V. or ević, N. Karabasil, and I. ekić. 2019. Comparison of a computer vision system vs. traditional colorimeter for color evaluation of meat products with various physical properties. Meat Sci. 148:5–12. https://doi.org/10.1016/j.meatsci.2018.09.015.

Troy, D. J., K. S. Ojha, J. P. Kerry, and B. K. Tiwari. 2016. Sustainable and consumer-friendly emerging technologies for application within the meat industry: An overview. Meat Sci. 120:2–9. https://doi.org/10.1016/j.meatsci.2016.04.002.

Uttaro, B., S. Zawadski, I. Larsen, and M. Juárez. 2021. An image analysis approach to identification and measurement of marbling in the intact pork loin. Meat Sci. 179:108549. https://doi.org/10.1016/j.meatsci.2021.108549.

Vargas, F. M. J., T. Fernandes, A. T. de Matos, A. R. M. Fernandes, L. G. C. Alves, J. A. Rossatti, G. D. V. Britez, and N. G. T. Zagonel. 2021. Evaluator effect on the ultrasound measurement of subcutaneous fat deposition and loin eye area from weaning to slaughter lambs. Vet. World. 14:259–264. https://doi.org/10.14202/vetworld.2021.259-264.

Vázquez-Arellano, M., H. W. Griepentrog, D. Reiser, and D. S. Paraforos. 2016. 3-D Imaging systems for agricultural applications—A review. Sensors. 16:618. https://doi.org/10.3390/s16050618.

Velásquez, L., J. P. Cruz-Tirado, R. Siche, and R. Quevedo. 2017. An application based on the decision tree to classify the marbling of beef by hyperspectral imaging. Meat Sci. 133:43–50. https://doi.org/10.1016/j.meatsci.2017.06.002.

Wang, W., Y. Peng, H. Sun, X. Zheng, and W. Wei. 2018a. Real-time inspection of pork quality attributes using dual-band spectroscopy. J. Food Eng. 237:103–109. https://doi.org/10.1016/j.jfoodeng.2018.05.022.

Wang, W., Y. Peng, H. Sun, X. Zheng, and W. Wei. 2018b. Spectral detection techniques for non-destructively monitoring the quality, safety, and classification of fresh red meat. Food Anal. Method. 11:2707–2730. https://doi.org/10.1007/s12161-018-1256-4.

Wang, C., S. Wang, X. He, L. Wu, Y. Li, and J. Guo. 2020a. Combination of spectra and texture data of hyperspectral imaging for prediction and visualization of palmitic acid and oleic acid contents in lamb meat. Meat Sci. 169:108194. https://doi.org/10.1016/j.meatsci.2020.108194.

Wang, W., C. Zhang, F. Zhang, Y. Peng, and J. Sun. 2020b. Real-time and online inspection of multiple pork quality parameters using dual-band visible/near-infrared spectroscopy. Food Anal. Method. 13:1764–1773. https://doi.org/10.1007/s12161-020-01801-8.

Weng, S., B. Guo, P. Tang, X. Yin, F. Pan, J. Zhao, L. Huang, and D. Zhang. 2020. Rapid detection of adulteration of minced beef using Vis/NIR reflectance spectroscopy with multivariate methods. Spectrochim. Acta A. 230:118005. https://doi.org/10.1016/j.saa.2019.118005.

Xiong, Z., D. W. Sun, H. Pu, W. Gao, and Q. Dai. 2017. Applications of emerging imaging techniques for meat quality and safety detection and evaluation: A review. Crit. Rev. Food Sci. 57:755–768. https://doi.org/10.1080/10408398.2014.954282.

Xiong, Z., D.-W. Sun, X.-A. Zeng, and A. Xie. 2014. Recent developments of hyperspectral imaging systems and their applications in detecting quality attributes of red meats: A review. J. Food Eng. 132:1–13. https://doi.org/10.1016/j.jfoodeng.2014.02.004.

Yancey, J. W., J. K. Apple, J. F. Meullenet, and J. T. Sawyer. 2010. Consumer responses for tenderness and overall impression can be predicted by visible and near-infrared spectroscopy, Meullenet-Owens razor shear, and Warner-Bratzler shear force. Meat Sci. 85:487–492. https://doi.org/10.1016/j.meatsci.2010.02.020.

Yang, D., and Y. Ying. 2011. Applications of Raman spectroscopy in agricultural products and food analysis: a review. Appl. Spectrosc. Rev. 46:539–560. https://doi.org/10.1080/05704928.2011.593216.

Yang, H., D. L. Hopkins, Y. Zhang, L. Zhu, P. Dong, X. Wang, Y. Mao, X. Luo, and S. M. Fowler. 2020. Preliminary investigation of the use of Raman spectroscopy to predict beef spoilage in different types of packaging. Meat Sci. 165:108136. https://doi.org/10.1016/j.meatsci.2020.108136.

Yang, L., T. Wu, Y. Liu, J. Zou, Y. Huang, S. Babu V, and L. Lin. 2018. Rapid identification of pork adulterated in the beef and mutton by infrared spectroscopy. J. Spectrosc. 2018:1–10. https://doi.org/10.1155/2018/2413874.

Yao, X., F. Cai, P. Zhu, H. Fang, J. Li, and S. He. 2019. Non-invasive and rapid pH monitoring for meat quality assessment using a low-cost portable hyperspectral scanner. Meat Sci. 152:73–80. https://doi.org/10.1016/j.meatsci.2019.02.017.

Yu, W., C. Wang, L. Qiao, S. Wang, and X. He. 2020. Construction of PLSR prediction model for detecting color of Jingyuan yellow beef by hyperspectral technique. Acta Agriculturae Zhejiangensis. 32:527–533. https://doi.org/10.3969/j.issn.1004-1524.2020.03.19.

Yuan, R., G. Liu, J. He, C. Ma, L. Cheng, N. Fan, J. Ban, Y. Li, and Y. Sun. 2020. Determination of metmyoglobin in cooked tan mutton using Vis/NIR hyperspectral imaging system. J. Food Sci. 85:1403–1410. https://doi.org/10.1111/1750-3841.15137.

Zhao, H.-T., Y.-Z. Feng, W. Chen, and G.-F. Jia. 2019. Application of invasive weed optimization and least square support vector machine for prediction of beef adulteration with spoiled beef based on visible near-infrared (Vis-NIR) hyperspectral imaging. Meat Sci. 151:75–81. https://doi.org/10.1016/j.meatsci.2019.01.010.

Zhao, X., H. Zhuang, S.-C. Yoon, Y. Dong, W. Wang, and W. Zhao. 2017. Electrical impedance spectroscopy for quality assessment of meat and fish: a review on basic principles, measurement methods, and recent advances. J. Food Quality. 2017:1–16. https://doi.org/10.1155/2017/6370739.

Zheng, X., Y. Li, W. Wei, and Y. Peng. 2019. Detection of adulteration with duck meat in minced lamb meat by using visible near-infrared hyperspectral imaging. Meat Sci. 149:55–62. https://doi.org/10.1016/j.meatsci.2018.11.005.

Zhu, R., Z. Bai, Y. Qiu, M. Zheng, J. Gu, and X. Yao. 2021. Comparison of mutton freshness grade discrimination based on hyperspectral imaging, near infrared spectroscopy and their fusion information. J. Food Process Eng. 44:e13642. https://doi.org/10.1111/jfpe.13642.